A mixed formulation for the direct approximation of the control of minimal L^2-norm for linear type wave equations

Nicolae Cindea, Arnaud Munch

A mixed formulation for the direct approximation of the control of minimal L^2-norm for linear type wave equations

Nicolae Cîndea* Arnaud Münch*

August 23, 2013

Abstract

This paper deals with the numerical computation of null controls for the wave equation with a potential. The goal is to compute approximations of controls that drive the solution from a prescribed initial state to zero at a large enough controllability time. In [*Cindea, Fernandez-Cara & Münch, Numerical controllability of the wave equation through primal methods and Carleman estimates, 2013*], a so called primal method is described leading to a strongly convergent approximation of boundary controls : the controls minimize quadratic weighted functionals involving both the control and the state and are obtained by solving the corresponding optimality condition. In this work, we adapt the method to approximate the control of minimal square-integrable norm. The optimality conditions of the problem are reformulated as a mixed formulation involving both the state and his adjoint. We prove the well-posedeness of the mixed formulation (in particular the inf-sup condition) then discuss several numerical experiments. The approach covers both the boundary and the inner controllability. For simplicity, we present the approach in the one dimensional case.

Keywords: Linear wave equation, null controllability, finite element methods, Mixed formulation.

Mathematics Subject Classification (2010)- 35L10, 65M12, 93B40.

Contents

*Laboratoire de Mathématiques, Université Blaise Pascal (Clermont-Ferand 2), UMR CNRS 6620, Campus de Cézeaux, 63177, Aubière, France. E-mails: nicolae.cindea@math.univ-bpclermont.fr, arnaud.munch@math.univ-bpclermont.fr.

1 Introduction. The null controllability problem

We are concerned in this work with the null controllability for the 1D wave equation with a potential. Let us explain our motivation for the boundary case for which the state equation is the following:

$$\begin{cases} y_{tt} - (c(x)y_x)_x + d(x,t)y = 0, & (x,t) \in (0,1)\times(0,T) \\ y(0,t) = 0, \qquad y(1,t) = v(t), & t \in (0,T) \\ y(x,0) = y_0(x), \qquad y_t(x,0) = y_1(x), & x \in (0,1). \end{cases} \tag{1}$$

Here, $T > 0$ and we assume that $c \in C^3([0,1])$ with $c(x) \geq c_0 > 0$ in $[0,1]$, $d \in L^\infty((0,1)\times(0,T))$, $y_0 \in L^2(0,1)$ and $y_1 \in H^{-1}(0,1)$; $v = v(t)$ is the *control* (a function in $L^2(0,T)$) and $y = y(x,t)$ is the associated state.

In the sequel, for any $\tau > 0$ we denote by Q_τ and Σ_τ the sets $(0,1)\times(0,\tau)$ and $\{0,1\}\times(0,\tau)$, respectively. We also use the following notation:

$$L\,y := y_{tt} - (c(x)y_x)_x + d(x,t)y. \tag{2}$$

For any $(y_0, y_1) \in \boldsymbol{Y} := L^2(0,1)\times H^{-1}(0,1)$ and any $v \in L^2(0,T)$, there exists exactly one solution y to (1), with the following regularity:

$$y \in C^0([0,T]; L^2(0,1)) \cap C^1([0,T]; H^{-1}(0,1)) \tag{3}$$

(see for instance [27]). The null controllability problem for (1) at time T is the following: for each $(y_0, y_1) \in \boldsymbol{Y}$, find $v \in L^2(0,T)$ such that the corresponding solution to (1) satisfies

$$y(\cdot\,,T) = 0, \quad y_t(\cdot\,,T) = 0 \quad \text{in} \quad (0,1). \tag{4}$$

It is well known that (1) is null-controllable at any *large* time $T > T^\star$ for some $T^\star$ that depends on c (for instance, see [2, 27] for $c \equiv 1$ and $d \equiv 0$ leading to $T^\star = 2$ and see [33] for a general situation). Moreover, as a consequence of the *Hilbert Uniqueness Method* of J.-L. Lions [27], the null controllability of (1) is equivalent to an observability inequality for the associated adjoint problem.

In the last two decades, a large number of works has been concerned with the (numerical) approximation of null controls for wave type equations. Since controllability holds in L^2, the approximation of the minimal L^2-norm control (refereed by some authors as the HUM control) has focused most of the attention : the problem reads

$$\begin{cases} \text{Minimize} \quad J(y,v) = \dfrac{1}{2}\displaystyle\int_0^T |v(t)|^2\,dt \\ \text{Subject to} \quad (y,v) \in \mathcal{C}(y_0, y_1; T) \end{cases} \tag{5}$$

where $\mathcal{C}(y_0, y_1; T)$ denotes the linear manifold

$$\mathcal{C}(y_0, y_1; T) = \{\,(y,v) : v \in L^2(0,T),\ y \text{ solves (1) and satisfies (4)}\,\}.$$

The earlier contribution is due to Glowinski and Lions in [19] (updated in [20]) and relies on duality arguments. Duality allows to replace the original constrained minimization problem by an

unconstrained and *a priori* easier minimization (dual) problem. We define $\boldsymbol{V} = H_0^1(0,1)\times L^2(0,1)$. The dual problem associated with (5) is :

$$\min_{(\varphi_0,\varphi_1)\in\boldsymbol{V}} J^\star(\varphi_0,\varphi_1) = \frac{1}{2}\int_0^T |c(1)\varphi_x(1,t)|^2 dt + \int_0^1 y_0(x)\varphi_t(x,0)dx - \langle y_1, \varphi(\cdot,0)\rangle_{H^{-1},H_0^1} \tag{6}$$

where the variable φ solves the backward wave equation :

$$L\varphi = 0 \quad \text{in} \quad Q_T, \qquad \varphi = 0 \quad \text{on} \quad \Sigma_T; \quad (\varphi(\cdot,T),\varphi_t(\cdot,T)) = (\varphi_0,\varphi_1). \tag{7}$$

The coercivity of $J^\star$ - called the conjugate functional of J - is the consequence of the following estimate : there exists $k_T > 0$ such that

$$\|\varphi(\cdot,0),\varphi_t(\cdot,0)\|_{\boldsymbol{V}}^2 \le k_T \|c(1)\varphi_x(1,\cdot)\|_{L^2(0,T)}^2, \quad \forall(\varphi_0,\varphi_1)\in\boldsymbol{V} \tag{8}$$

where $(\varphi_0,\varphi_1,\varphi)$ solves (7). This estimate, refereed in the literature as an *observability inequality*, holds true if T is large enough.

At the level of the approximation, the minimization of $J^\star$ requires to find a finite dimensional and conformal approximation of $\boldsymbol{V}$ such that the corresponding discrete adjoint solution satisfies (7), which is in general impossible for polynomial piecewise approximation. In practice, the trick initially described in [19], consists first to introduce a discrete and consistent approximation of (1) and then minimize the corresponding discrete conjugate functional. But this requires to prove uniform discrete observability inequalities that turn out to be not satisfied when very standard approximations (for instance based on finite differences on uniform meshes) are used. This is due to some spurious high frequencies components generated by the approximation which can not be controlled in a uniform time (with respect to the discretization parameters). This observation has raised many developments in order to get so-called uniform observable (or equivalently controllable) approximation. We mention the references [8, 15, 21, 22, 24, 28, 30] and we refer to [1, 4, 26] for some numerical realizations in 2D based on spectral methods. As far as we know, the determination of discrete observability inequalities is still open in the general case (non uniform mesh, wave equation with non constant coefficient, etc).

In contrast to these works where solutions of the discrete wave equations are exactly controlled to zero, we mention [12, 31] based on Russell's approach where convergent approximations of an exact control (not necessarily the HUM control) are build.

In [11], a different - so-called primal approach - allowing more general results has been used and consists to solve directly optimality conditions: specifically, the following general extremal problem is considered

$$\begin{cases} \text{Minimize} \quad J(y,v) = \dfrac{1}{2}\displaystyle\iint_{Q_T} \rho^2|y|^2\,dx\,dt + \frac{1}{2}\int_0^T \rho_0^2|v|^2\,dt \\ \text{Subject to} \quad (y,v)\in\mathcal{C}(y_0,y_1;T). \end{cases} \tag{9}$$

The weights ρ and ρ_0 are strictly positive, continuous and uniformly bounded from below by a positive constant in Q_T and $(0,T)$, respectively. For c in the class $\mathcal{A}(x_0,c_0)$ and T large enough, greater than $T^\star(c)$ (both defined in Section 2), the extremal problem (9) is well-posed. Moreover, defining the Hilbert space P as the completion of the linear space $P_0 = \{q\in C^\infty(\overline{Q_T}) : q = 0 \text{ on } \Sigma_T\}$ with respect to the scalar product

$$(p,q)_P := \iint_{Q_T} \rho^{-2} Lp\,Lq\,dx\,dt + \int_0^T \rho_0^{-2}\,c(1)^2\,p_x(1,t)\,q_x(1,t)\,dt, \tag{10}$$

we may obtain the following characterization of the optimal pair (y,v) in term of an additional variable $p\in P$ as follows:

$$y = -\rho^{-2}Lp \quad \text{in} \quad Q_T, \qquad v = -(c(x)\rho_0^{-2}p_x)\big|_{x=1} \quad \text{in} \quad (0,T); \tag{11}$$

$p \in P$ is the unique solution to the following variational equality:

$$(p,q)_P = \int_0^1 y_0(x)\, q_t(x,0)\, dx - \langle y^1, q(\cdot,0)\rangle_{H^{-1},H_0^1}, \quad \forall q \in P. \tag{12}$$

Here and in the sequel, we use the following duality pairing:

$$\langle y^1, q(\cdot,0)\rangle_{H^{-1},H_0^1} = \int_0^1 \frac{\partial}{\partial x}((-\Delta)^{-1} y_1)(x)\, q_x(x,0)\, dx,$$

where $-\Delta$ is the Dirichlet Laplacian in $(0,1)$. We refer the reader to [11] for the details. The search of a control v in the manifold $\mathcal{C}(y_0, y_1, T)$ is reduced to solve the (elliptic) variational formulation (12). The approximation of the solution of (12) is performed in the framework of the finite element theory through a discretization of the space-time domain Q_T. In practice, an approximation p_h of p is obtained in a direct way by inverting a symmetric positive definite matrix, in contrast with the iterative (and possibly divergent) methods used within dual methods. Moreover, a major advantage of this approach is that a conformal approximation, say P_h of P, leads to the strong convergence of p_h toward p in P, and consequently from (11), to a strong convergence in L^2 of $v_h := -(c(x)\rho_0^{-2} p_{h,x})\big|_{x=1}$ toward v, a null control for (1). It is worth to mention that, for any $h > 0$, as in the works [12, 31] mentioned earlier, v_h is not *a priori* an exact control for any finite dimensional system but an approximation for the L^2-norm of the control v.

The variational formulation (12) derived from the optimality conditions (11) is obtained assuming that the weights ρ and ρ_0 are strictly positive in Q_T and $(0,T)$ respectively. In particular, this approach does not apply for the control of minimal L^2-norm, for which simply $\rho := 0$ and $\rho_0 := 1$. The main reason of the present work is to adapt this approach to cover the case $\rho := 0$ and therefore obtain directly a strong convergent approximation v_h of the control of minimal L^2-norm.

The paper is organized as follows. In Section 2, we recall the definition of the admissible set $\mathcal{A}(x_0, c_0)$ for the function c and of the minimal time $T^\star(c)$ determined in [11] then we associate to the dual problem (6) an equivalent mixed formulation which relies on the optimality conditions associated to the problem (5). We then show the well-posedness of this mixed formulation, in particular we check the inf-sup condition. The mixed formulation allows to approximate simultaneously the dual variable and the primal one, controlled solution of (1). Interestingly, we also derive an extremal problem in the primal variable y only. Section 3 is devoted to the distributed case for which the strategy also applies. Section 4 is devoted to the numerical approximation of the mixed formulation as well as numerical experiments, both in the boundary and inner case. Eventually, Section 5 concludes with some perspectives : in particular, we highlight that the variational approach is very appropriate to consider inner control distributed on time dependent support, an issue recently considered in [6].

2 Control of minimal L^2-norm: a mixed reformulation

We present in this section a mixed formulation based on the optimality conditions associated to the extremal problem (5). The starting point is the dual problem recalled in the introduction. Preliminary, we precise the minimal controllability time $T^\star$.

We introduce the set

$$\begin{aligned}\mathcal{A}(x_0,c_0) = \Big\{ & c \in C^3([0,1]) : c(x) \geq c_0 > 0, \\ & -\min_{[0,1]} \Big(c(x) + (x-x_0)c_x(x)\Big) < \min_{[0,1]} \Big(c(x) + \frac{1}{2}(x-x_0)c_x(x)\Big) \Big\},\end{aligned} \tag{13}$$

where $x_0 < 0$ and c_0 is a positive constant. This set is non empty and contains in particular the constant function $c := c_0$. The following result holds.

PROPOSITION 2.1 ([11]) *Let us assume that $x_0 < 0$, $c_0 > 0$ and $c \in \mathcal{A}(x_0, c_0)$. Let $\beta > 0$ be a positive number with*

$$-\min_{[0,1]}\Big(c(x)+(x-x_0)c_x(x)\Big) < \beta < \min_{[0,1]}\Big(c(x)+\frac{1}{2}(x-x_0)c_x(x)\Big)$$

and let us consider the function $\phi(x,t) := |x-x_0|^2 - \beta t^2 + M_0$ where M_0 is such that $\phi(x,t) \geq 1$ for all $(x,t) \in (0,1)\times(-T,T)$. Then, for any $\lambda > 0$ we set $g(x,t) := e^{\lambda\phi(x,t)}$. Finally, let us assume that

$$T > \frac{1}{\beta}\max_{[0,1]} c(x)^{1/2}(x-x_0). \tag{14}$$

Then there exist positive constants s_0 and M, only depending on x_0, c_0, $\|c\|_{C^3([0,1])}$, $\|d\|_{L^\infty(Q_T)}$ and T, such that, for all $s > s_0$, one has

$$\begin{aligned} &s\int_{-T}^{T}\int_0^1 e^{2sg}\left(|w_t|^2+|w_x|^2\right)\,dx\,dt + s^3\int_{-T}^{T}\int_0^1 e^{2sg}|w|^2\,dx\,dt \\ &\quad\leq M\int_{-T}^{T}\int_0^1 e^{2sg}|Lw|^2\,dx\,dt + Ms\int_{-T}^{T} e^{2sg}|w_x(1,t)|^2\,dt \end{aligned} \tag{15}$$

for any $w \in L^2(-T,T;H_0^1(0,1))$ satisfying $Lw \in L^2((0,1)\times(-T,T))$ and $w_x(1,\cdot) \in L^2(-T,T)$.

Then, for any $c \in \mathcal{A}(x_0,c_0)$, we define $T^\star(c)$ as follows :

$$T^\star(c) := \frac{2}{\beta}\max_{[0,1]} c(x)^{1/2}(x-x_0). \tag{16}$$

with β as in Proposition 2.1.

Proposition 2.1 allows to show in particular that for any $c \in \mathcal{A}$ and any $T > T^\star(c)$, there exists a positive constant $k_T = k_T(c)$ such that the estimate (8) holds. We refer to [11] for details. The minimization of $J^\star$ is then well-posed and if $(\hat\varphi_0, \hat\varphi_1)$ denotes the minimizer of $J^\star$, the control of minimal L^2-norm is given by

$$v = c(1)\hat\varphi_x(1,\cdot) \quad \text{in} \quad (0,T). \tag{17}$$

The extremal problem $\min_{(\varphi_0,\varphi_1)\in \boldsymbol{V}} J^\star(\varphi_0,\varphi_1)$ is usually called the dual problem associated to (5).

Remark 1 *The inequality (8) can also be obtained directly by the multiplier method (see [33]) and requires T to be large enough. Note that, when $c(x) \equiv c_0$, the assumption (14) simply reads $T > \frac{2(1-x_0)}{\sqrt{c_0}} > \frac{2}{\sqrt{c_0}}$ which is optimal.* □

2.1 Mixed reformulation of the controllability problem

In order to avoid the minimization of the functional $J^\star$ with respect to the initial data (φ_0,φ_1), we now present a direct way to approximate the HUM control, in the spirit of the primal approach recalled in the introduction and developed in [11].

Since the variable φ, solution of (7), is completely and uniquely determined by the data (φ_0,φ_1), the main idea of the reformulation is to keep φ as main variable and consider the following extremal problem:

$$\min_{\varphi\in W}\hat J^\star(\varphi) = \frac{1}{2}\int_0^T |c(1)\varphi_x(1,t)|^2 dt + \int_0^1 y_0(x)\varphi_t(x,0)dx - \langle y_1, \varphi(\cdot,0)\rangle_{H^{-1},H_0^1}, \tag{18}$$

where

$$W = \left\{\varphi \in L^2(Q_T),\ \varphi = 0 \text{ on } \Sigma_T \text{ such that } L\varphi = 0 \in L^2(Q_T) \text{ and } \varphi_x(1,\cdot) \in L^2(0,T)\right\}.$$

W is an Hilbert space endowed with the inner product

$$(\varphi,\overline{\varphi})_W=\int_0^T c(1)\varphi_x(1,t)\overline{\varphi}_x(1,t)\,dt+\eta\iint_{Q_T}L\varphi L\overline{\varphi}\,dx\,dt,\quad\forall\varphi,\overline{\varphi}\in W,$$

for any fixed $\eta>0$. We denote $\|\cdot\|_W$ the associated norm such that

$$\|\varphi\|_W^2=\int_0^T|c(1)\varphi_x(1,t)|^2dt+\eta\|L\varphi\|^2_{L^2(Q_T)},\quad\forall\varphi\in W. \tag{19}$$

The minimization of $\hat{J}^\star$ is evidently equivalent to the minimization of $J^\star$ over $\boldsymbol{V}$. Remark that from (8) the property $\varphi\in W$ implies that $(\varphi(\cdot,0),\varphi_t(\cdot,0))\in\boldsymbol{V}$, so that the functional $\hat{J}^\star$ is well-defined over W.

The main variable is now φ submitted to the constraint equality (in $L^2(Q_T)$) $L\varphi=0$. This constraint is addressed by introducing a mixed formulation. We define the space Φ larger than W by

$$\Phi=\left\{\varphi\in L^2(Q_T),\ \varphi=0\text{ on }\Sigma_T\text{ such that }L\varphi\in L^2(Q_T)\text{ and }\varphi_x(1,\cdot)\in L^2(0,T)\right\}.$$

Φ is endowed with the same norm than W.

Then, we consider the following mixed formulation : find $(\varphi,\lambda)\in\Phi\times L^2(Q_T)$ solution of

$$\left\{\begin{array}{rcll} a(\varphi,\overline{\varphi})+b(\overline{\varphi},\lambda) &=& l(\overline{\varphi}), & \forall\overline{\varphi}\in\Phi\\ b(\varphi,\overline{\lambda}) &=& 0, & \forall\overline{\lambda}\in L^2(Q_T),\end{array}\right. \tag{20}$$

where

$$a:\Phi\times\Phi\to\mathbb{R},\quad a(\varphi,\overline{\varphi})=\int_0^T c(1)\varphi_x(1,t)\overline{\varphi}_x(1,t)dt \tag{21}$$

$$b:\Phi\times L^2(Q_T)\to\mathbb{R},\quad b(\varphi,\lambda)=\iint_{Q_T}L\varphi(x,t)\lambda(x,t)dxdt \tag{22}$$

$$l:\Phi\to\mathbb{R},\quad l(\varphi)=-\int_0^1 y_0(x)\,\varphi_t(x,0)dx+\langle y_1,\varphi(\cdot,0)\rangle_{H^{-1},H_0^1}. \tag{23}$$

We have the following result :

THEOREM 2.1 *(i) The mixed formulation* (20) *is well-posed.*

(ii) The unique solution $(\varphi,\lambda)\in\Phi\times L^2(Q_T)$ is the unique saddle-point of the Lagrangian $\mathcal{L}:\Phi\times L^2(Q_T)\to\mathbb{R}$ defined by

$$\mathcal{L}(\varphi,\lambda)=\frac{1}{2}a(\varphi,\varphi)+b(\varphi,\lambda)-l(\varphi). \tag{24}$$

(iii) The optimal function φ is the minimizer of $\hat{J}^\star$ over Φ while the optimal function $\lambda\in L^2(Q_T)$ is the state of the controlled wave equation (1) *in the weak sense.*

PROOF - We easily check that the bilinear form a is continuous over $\Phi\times\Phi$, symmetric and positive and that the bilinear form b is continuous over $\Phi\times L^2(Q_T)$. Furthermore, assuming $c\in\mathcal{A}$ and $T>T^\star(c)$, the continuity of the linear form l over Φ is a direct consequence of the Carleman estimate (15) given by Proposition 2.1. Precisely, using the fact that the weight e^{2gs} (see (15)) is bounded and uniformly positive, we deduce from (15) that there exists a constant $C_0>0$ such that

$$\|\varphi(\cdot,0),\varphi_t(\cdot,0)\|^2_{H_0^1\times L^2}\le C_0\left(\|L\varphi\|^2_{L^2(Q_T)}+\|c(1)\varphi_x(1,\cdot)\|^2_{L^2(0,T)}\right),\quad\forall\varphi\in\Phi. \tag{25}$$

Therefore, the well-posedness of the mixed formulation is a consequence of the following two properties (see [5]):

- a is coercive on $\mathcal{N}(b)$, where $\mathcal{N}(b)$ denotes the kernel of b :

$$\mathcal{N}(b) = \{\varphi \in \Phi \text{ such that } b(\varphi, \lambda) = 0 \text{ for every } \lambda \in L^2(Q_T)\}.$$

- b satisfies the usual "inf-sup" condition over $\Phi \times L^2(Q_T)$: there exists $\delta > 0$ such that

$$\inf_{\lambda \in L^2(Q_T)} \sup_{\varphi \in \Phi} \frac{b(\varphi, \lambda)}{\|\varphi\|_\Phi \|\lambda\|_{L^2(Q_T)}} \geq \delta. \tag{26}$$

From the definition of a, the first point is clear : for all $\varphi \in \mathcal{N}(b) = W$, $a(\varphi, \varphi) = \|\varphi\|_W^2$. Let us check the inf-sup condition. For any fixed $\lambda_0 \in L^2(Q_T)$, we define the (unique) element φ_0 such that $L\varphi_0 = \lambda_0$ and such that $\varphi(\cdot, 0) = 0$ in $H_0^1(0,1)$ and $\varphi_t(\cdot, 0) = 0$ in $L^2(0,1)$. φ_0 is therefore solution of the wave equation with source term $\lambda_0 \in L^2(Q_T)$, null Dirichlet boundary condition and zero initial state. Since $\lambda_0 \in L^2(Q_T)$, then $\varphi_{0,x}(1,\cdot) \in L^2(0,T)$: precisely, using the multipliers method (see, for instance, Chapter 1 in [27]), there exists a constant $C_{\Omega,T} > 0$ such that the solution φ_0 of the wave equation with source term λ_0 satisfies the so-called direct equality

$$\int_0^T |c(1)\varphi_{0,x}(1,t)|^2 dt \leq C_{\Omega,T}\, c^2(1) \|\lambda_0\|^2_{L^2(Q_T)}. \tag{27}$$

Consequently, $\varphi_0 \in \Phi$. In particular, we have $b(\varphi_0, \lambda_0) = \|\lambda_0\|^2_{L^2(Q_T)}$ and

$$\sup_{\varphi \in \Phi} \frac{b(\varphi, \lambda_0)}{\|\varphi\|_\Phi \|\lambda_0\|_{L^2(Q_T)}} \geq \frac{b(\varphi_0, \lambda_0)}{\|\varphi_0\|_\Phi \|\lambda_0\|_{L^2(Q_T)}} = \frac{\|\lambda\|^2_{L^2(Q_T)}}{\left(\int_0^T |c(1)\varphi_x(1,t)|^2 dt + \eta \|\lambda_0\|^2_{L^2(Q_T)}\right)^{\frac{1}{2}} \|\lambda_0\|_{L^2(Q_T)}}.$$

Combining the above two inequalities, we obtain

$$\sup_{\varphi_0 \in \Phi} \frac{b(\varphi_0, \lambda_0)}{\|\varphi_0\|_\Phi \|\lambda_0\|_{L^2(Q_T)}} \geq \frac{1}{\sqrt{C_{\Omega,T} c^2(1) + \eta}}$$

and, hence, (26) holds with $\delta = \left(C_{\Omega,T} c^2(1) + \eta\right)^{-\frac{1}{2}}$.

The point (ii) is due to the symmetry and to the positivity of the bilinear form a. (iii). The equality $b(\varphi, \lambda) = 0$ for all $\lambda \in L^2(Q_T)$ implies that $L\varphi = 0$ as an $L^2(Q_T)$ function, so that if $(\varphi, \lambda) \in \Phi \times L^2(Q_T)$ solves the mixed formulation, then $\varphi \in W$ and $\mathcal{L}(\varphi, \lambda) = \hat{J}^\star(\varphi)$. Finally, the first equation of the mixed formulation reads as follows :

$$\int_0^T c(1)\varphi_x(1,t)\, \overline{\varphi}_x(1,t) dt + \iint_{Q_T} L\overline{\varphi}(x,t)\, \lambda(x,t)\, dx\, dt = l(\overline{\varphi}), \quad \forall \overline{\varphi} \in \Phi,$$

or equivalently, since the control is given by $v = c(1)\varphi_x(1,\cdot)$,

$$\int_0^T v(t)\, \overline{\varphi}_x(1,t) dt + \iint_{Q_T} L\overline{\varphi}(x,t)\, \lambda(x,t)\, dx\, dt = l(\overline{\varphi}), \quad \forall \overline{\varphi} \in \Phi.$$

But this means that $\lambda \in L^2(Q_T)$ is solution of the wave equation in the transposition sense. Since $(y_0, y_1) \in L^2(0,1) \times H^{-1}(0,1)$ and $v \in L^2(0,T)$, λ must coincide with the unique weak solution to (1). □

Therefore, Theorem 2.1 reduces the search of the HUM control to the resolution of the mixed formulation (20), or equivalently the search of the saddle point for $\mathcal{L}$. In general, it is very convenient (actually in the case considered here, it is necessary) to "augment" the Lagrangien (see [17]), and consider instead the Lagrangien $\mathcal{L}_r$ defined for any $r > 0$ by

$$\begin{cases} \mathcal{L}_r(\varphi, \lambda) = \dfrac{1}{2} a_r(\varphi, \varphi) + b(\varphi, \lambda) - l(\varphi), \\ a_r(\varphi, \varphi) = a(\varphi, \varphi) + r \displaystyle\iint_{Q_T} |L\varphi|^2\, dx\, dt. \end{cases}$$

Since $a(\varphi, \varphi) = a_r(\varphi, \varphi)$ on W, the lagrangian $\mathcal{L}$ and $\mathcal{L}_r$ share the same saddle-point.

2.2 Dual problem of the extremal problem (18)

The mixed formulation allows to solve simultaneously the dual variable φ, argument of the conjugate functional (18), and the Lagrange multiplier λ. Since λ turns out to be the controlled state of (1), we may qualify λ as the primal variable of the problem. We derive in this section the corresponding extremal problem involving only that variable λ.

For any $r > 0$, let us define the linear operator A_r from $L^2(Q_T)$ into $L^2(Q_T)$ by

$$A_r\lambda := L\varphi, \quad \forall \lambda \in L^2(Q_T)$$

where $\varphi \in \Phi$ is the unique solution to

$$a_r(\varphi, \overline{\varphi}) = b(\overline{\varphi}, \lambda), \quad \forall \overline{\varphi} \in \Phi. \tag{28}$$

Notice that the assumption $r > 0$ is necessary here in order to guarantee the well-posedness of (28). Precisely, for any $r > 0$, the form a_r defines a norm equivalent to the norm on Φ (see (19)).

We have the following important lemma :

LEMMA 2.1 *For any $r > 0$, the operator A_r is a strongly elliptic, symmetric isomorphism from $L^2(Q_T)$ into $L^2(Q_T)$.*

PROOF- From the definition of a_r, we easily get that $\|A_r\lambda\|_{L^2(Q_T)} \leq r^{-1}\|\lambda\|_{L^2(Q_T)}$ and the continuity of A_r. Next, consider any $\lambda' \in L^2(Q_T)$ and denote by φ' the corresponding unique solution of (28) so that $A_r\lambda' := L\varphi'$. Relation (28) with $\overline{\varphi} = \varphi'$ then implies that

$$\iint_{Q_T} (A_r\lambda')\lambda \, dx \, dt = a_r(\varphi, \varphi') \tag{29}$$

and therefore the symmetry and positivity of A_r. The last relation with $\lambda' = \lambda$ and the Carleman estimate (25) imply that A_r is also positive definite.

Finally, let us check the strong ellipticity of A_r, equivalently that the bilinear functional $(\lambda, \lambda') \to \iint_{Q_T}(A_r\lambda)\lambda' \, dx \, dt$ is $L^2(Q_T)$-elliptic. Thus we want to show that

$$\iint_{Q_T} (A_r\lambda)\lambda \, dx \, dt \geq C\|\lambda\|^2_{L^2(Q_T)}, \quad \forall \lambda \in L^2(Q_T) \tag{30}$$

for some positive constant C. Suppose that (30) does not hold; there exists then a sequence $\{\lambda_n\}_{n\geq 0}$ of $L^2(Q_T)$ such that

$$\|\lambda_n\|_{L^2(Q_T)} = 1, \quad \forall n \geq 0, \qquad \lim_{n\to\infty} \iint_{Q_T} (A_r\lambda_n)\lambda_n \, dx \, dt = 0.$$

Let us denote by φ_n the solution of (28) corresponding to λ_n. From (29), we then obtain that

$$\lim_{n\to\infty} \|L\varphi_n\|_{L^2(Q_T)} = 0, \qquad \lim_{n\to\infty} \|\varphi_{n,x}(1,\cdot)\|_{L^2(0,T)} = 0 \tag{31}$$

and thus $\lim_{n\to\infty} \iint_{Q_T} L\varphi \, \lambda_n \, dx \, dt = 0$ for all $\varphi \in \Phi$ (and so the $L^2(Q_T)$-weak-convergence of λ_n toward 0).

From (28) with $\varphi = \varphi_n$ and λ_n, we have

$$\iint_{Q_T} (rL\varphi_n - \lambda_n)L\overline{\varphi} \, dx \, dt + \int_0^T c(1)\varphi_{n,x}(1,\cdot)\overline{\varphi}_x(1,\cdot) \, dt = 0, \quad \forall \overline{\varphi} \in \Phi. \tag{32}$$

We define the sequence $\{\overline{\varphi}_n\}_{n\geq 0}$ as follows :

$$\begin{cases} L\overline{\varphi}_n = r\, L\varphi_n - \lambda_n, & \text{in} \quad Q_T, \\ \overline{\varphi}_n(0,\cdot) = \overline{\varphi}_n(1,\cdot) = 0, & \text{in} \quad (0,T), \\ \overline{\varphi}_n(\cdot,0) = \overline{\varphi}_{n,t}(\cdot,0) = 0, & \text{in} \quad (0,1), \end{cases}$$

so that, for all n, $\overline{\varphi}_n$ is the solution of the wave equation with zero initial data and source term $r\,L\varphi_n - \lambda_n$ in $L^2(Q_T)$. Using again (27), we get $\|\overline{\varphi}_{n,x}(1,\cdot)\| \leq C_{\Omega,T}\|rL\varphi_n - \lambda_n\|_{L^2(Q_T)}$, so that $\overline{\varphi}_n \in \Phi$. Then, using (32), we get

$$\|rL\varphi_n - \lambda_n\|_{L^2(Q_T)} \leq C_{\Omega,T}\|\varphi_{n,x}(1,\cdot)\|_{L^2(0,T)}.$$

Then, from (31), we conclude that $\lim_{n\to+\infty}\|\lambda_n\|_{L^2(Q_T)} = 0$ leading to a contradiction and to the strong ellipticity of the operator A_r. □

The introduction of the operator A_r is motivated by the following proposition :

PROPOSITION 2.2 *For any r¿0, let $\varphi_0 \in \Phi$ be the unique solution of*

$$a_r(\varphi_0, \overline{\varphi}) = l(\overline{\varphi}), \quad \forall \overline{\varphi} \in \Phi$$

and let $J^{\star\star} : L^2(Q_T) \to L^2(Q_T)$ be the functional defined by

$$J^{\star\star}(\lambda) = \frac{1}{2}\iint_{Q_T}(A_r\lambda)\,\lambda\,dx\,dt - b(\varphi_0, \lambda).$$

The following equality holds :

$$\sup_{\lambda\in L^2(Q_T)}\inf_{\varphi\in\Phi}\mathcal{L}_r(\varphi,\lambda) = -\inf_{\lambda\in L^2(Q_T)}J^{\star\star}(\lambda) \quad + \mathcal{L}_r(\varphi_0, 0).$$

PROOF- For any $\lambda \in L^2(Q_T)$, let us denote by $\varphi_\lambda \in \Phi$ the minimizer of $\varphi \to \mathcal{L}_r(\varphi,\lambda)$; φ_λ satisfies the equation

$$a_r(\varphi_\lambda, \overline{\varphi}) + b(\overline{\varphi}, \lambda) = l(\overline{\varphi}), \quad \forall \overline{\varphi} \in \Phi$$

and can be decomposed as follows : $\varphi_\lambda = \psi_\lambda + \varphi_0$ where $\psi_\lambda \in \Phi$ solves

$$a_r(\psi_\lambda, \overline{\varphi}) + b(\overline{\varphi}, \lambda) = 0, \quad \forall \overline{\varphi} \in \Phi.$$

We then have

$$\begin{aligned}\inf_{\varphi\in\Phi}\mathcal{L}_r(\varphi,\lambda) &= \mathcal{L}_r(\varphi_\lambda,\lambda) = \mathcal{L}_r(\psi_\lambda+\varphi_0,\lambda)\\ &= \frac{1}{2}a_r(\psi_\lambda+\varphi_0,\psi_\lambda+\varphi_0) + b(\psi_\lambda+\varphi_0,\lambda) - l(\psi_\lambda+\varphi_0)\\ &:= X_1 + X_2 + X_3\end{aligned}$$

with

$$\begin{cases} X_1 = \dfrac{1}{2}a_r(\psi_\lambda,\psi_\lambda) + b(\psi_\lambda,\lambda) + b(\varphi_0,\lambda)\\ X_2 = a_r(\psi_\lambda,\varphi_0) - l(\psi_\lambda), \quad X_3 = \dfrac{1}{2}a_r(\varphi_0,\varphi_0) - l(\varphi_0). \end{cases}$$

From the definition of φ_0, $X_2 = 0$ while $X_3 = \mathcal{L}_r(\varphi_0, 0)$. Eventually, from the definition of ψ_λ,

$$X_1 = -\frac{1}{2}a_r(\psi_\lambda,\psi_\lambda) + b(\varphi_0,\lambda) = -\frac{1}{2}\iint_{Q_T}(A_r\lambda)\,\lambda\,dx\,dt + b(\varphi_0,\lambda)$$

and the result follows. □

From the ellipticity of the operator A_r, the minimization of the functional $J^{\star\star}$ over $L^2(Q_T)$ is well-posed. It is interesting to note that with this extremal problem involving only λ, we are coming to the primal variable, controlled solution of (1) (see Theorem 2.1, (iii)). Due to the constraint (4), the direct minimization of problem (5) with respect to the controlled state is usually avoided in practice. Here, any constraint equality is assigned to the variable λ.

From the symmetry and ellipticity of the operator A_r, the conjugate gradient algorithm is very appropriate to minimize $J^{\star\star}$, and consequently to solve the mixed formulation (20). The conjugate gradient algorithm reads as follows :

(i) Let $\lambda^0 \in L^2(Q_T)$ be a given function.

(ii) Compute $\overline{\varphi}_0 \in \Phi$ solution to

$$a_r(\overline{\varphi}^0, \overline{\varphi}) + b(\overline{\varphi}, \lambda^0) = l(\overline{\varphi}), \quad \forall \overline{\varphi} \in \Phi$$

and $g^0 = L\varphi^0$ then set $w^0 = g^0$.

(iii) For $n \geq 0$, assuming that λ^n, g^n and w^n are known, compute $\overline{\varphi}^n \in \Phi$ solution to

$$a_r(\overline{\varphi}^n, \overline{\varphi}) = b(\overline{\varphi}, g^n), \quad \forall \overline{\varphi} \in \Phi$$

and $\overline{g}^n = L\overline{\varphi}^n$ and then

$$\rho_n = \|g^n\|^2_{L^2(Q_T)} / \iint_{Q_T} \overline{g}^n w^n dxdt.$$

Update λ^n and g^n by

$$\lambda^{n+1} = \lambda^n - \rho_n w^n, \quad g^{n+1} = g^n - \rho^n \overline{g}^n.$$

If $\|g^{n+1}\|_{L^2(Q_T)} / \|g^0\|_{L^2(Q_T)} \leq \varepsilon$, take $\lambda = \lambda^{n+1}$. Else, compute

$$\gamma_n = \|g^{n+1}\|^2_{L^2(Q_T)} / \|g^n\|^2_{L^2(Q_T)}$$

and update w^n via

$$w^{n+1} = g^{n+1} + \gamma_n w^n.$$

Do $n = n + 1$ and return to step (iii).

As mentioned in [18] where this approach is discussed in length for Stokes and Navier-Stokes system, this algorithm can be viewed as a sophisticated version of Uzawa type algorithm.

Concerning the speed of convergence of the conjugate gradient algorithm (i)-(iii), it follows, for instance, from [13] that

$$\|\lambda^n - \lambda\|_{L^2(Q_T)} \leq 2\sqrt{\nu(A_r)} \left(\frac{\sqrt{\nu(A_r)} - 1}{\sqrt{\nu(A_r)} + 1} \right)^n \|\lambda^0 - \lambda\|_{L^2(Q_T)}, \quad \forall n \geq 1$$

where λ minimizes $J^{\star\star}$. $\nu(A_r) = \|A_r\| \|A_r^{-1}\|$ denotes the condition number of the operator A_r.

Eventually, once the above algorithm has converged we can compute $\varphi \in \Phi$ as solution of

$$a_r(\varphi, \overline{\varphi}) + b(\overline{\varphi}, \lambda) = l(\overline{\varphi}), \quad \forall \overline{\varphi} \in \Phi.$$

3 Mixed formulation for the distributed case

The mixed approach may be also used to address the inner situation, the main difference being the regularity of the initial data to be controlled. Let ω be a open and non empty subset of $(0,1)$ and 1_ω its characteristic function. We set $q_T = \omega \times (0,T)$ and recall that $\Sigma_T = \{0,1\} \times (0,T)$. For any initial data $(y_0, y_1) \in H_0^1(0,1) \times L^2(0,1)$ and any $v \in L^2(q_T)$, the boundary value problem

$$\begin{cases} Ly = v\, 1_\omega & \text{in} \quad Q_T, \\ y = 0 & \text{on} \quad \Sigma_T, \\ (y(\cdot,0), y_t(\cdot,0)) = (y_0, y_1) & \text{in} \quad \Omega \end{cases} \tag{33}$$

is well-posed and the solution y enjoys the regularity $y \in C^0([0,T]; H_0^1(0,1)) \cap C^1([0,T]; L^2(0,1))$. Again, the controllability problem for (33) consists in finding a control function $v \in L^2(q_T)$ such that (4) holds.

The dual formulation associated to the control of minimal L^2-norm for (33) is

$$\min_{(\varphi_0,\varphi_1)\in L^2(0,1)\times H^{-1}(0,1)} J^\star(\varphi_0,\varphi_1) = \frac{1}{2}\iint_{q_T} |\varphi|^2\,dx\,dt + < \varphi_1, y_0 >_{H^{-1}(0,1),H_0^1(0,1)} - \int_\Omega \varphi_0\, y_1\,dx$$

where the adjoint solution solves again the homogeneous adjoint equation (7). The dual formulation is well-posed as soon as T is large enough: this is given by the inner version of the estimate (8) (see [27]) :

$$\exists k_T > 0 \quad \text{such that} \quad \|\varphi(\cdot,0),\varphi_t(\cdot,0)\|_{L^2\times H^{-1}} \le k_T \|\varphi\|_{L^2(q_T)}, \quad \forall (\varphi_0,\varphi_1)\in L^2(0,1)\times H^{-1}(0,1)$$

where φ solves (7). As in the case of boundary control, since the solution of the adjoint system is completely determined by the initial data (φ_0,φ_1), we keep φ as the minimization variable and consider the extremal problem

$$\min_{\varphi\in W} \hat{J}^\star(\varphi) = \frac{1}{2}\iint_{q_T} |\varphi|^2\,dx\,dt + < \varphi_t(\cdot,0), y_0 >_{H^{-1}(0,1),H_0^1(0,1)} - \int_\Omega \varphi(\cdot,0)\, y_1\,dx, \tag{34}$$

where

$$W = \left\{\varphi\in L^2(q_T),\ \varphi = 0 \text{ on } \Sigma_T \text{ such that } L\varphi = 0 \in L^2(0,T;H^{-1}(0,1))\right\}.$$

Following the lines of Section 2.1, W is a Hilbert space endowed with the inner product

$$(\varphi,\overline{\varphi})_W = \iint_{q_T} \varphi(x,t)\overline{\varphi}(x,t)\,dx\,dt + \eta\int_0^T < L\varphi, L\overline{\varphi} >_{H^{-1}(0,1),H^{-1}(0,1)}\ dt,$$

for any fixed $\eta > 0$. We define

$$\Phi = \left\{\varphi\in L^2(q_T),\ \varphi = 0 \text{ on } \Sigma_T \text{ such that } L\varphi\in L^2(0,T;H^{-1}(0,1))\right\}$$

and consider the following mixed formulation : find $(\varphi,\lambda)\in\Phi\times L^2(0,T;H_0^1(0,1))$ solution of

$$\left\{\begin{array}{rcll} a(\varphi,\overline{\varphi}) + b(\overline{\varphi},\lambda) &=& l(\overline{\varphi}), & \forall\overline{\varphi}\in\Phi \\ b(\varphi,\overline{\lambda}) &=& 0, & \forall\overline{\lambda}\in L^2(0,T;H_0^1(0,1)), \end{array}\right. \tag{35}$$

where

$$a:\Phi\times\Phi\to\mathbb{R}, \quad a(\varphi,\overline{\varphi}) = \iint_{q_T}\varphi(x,t)\overline{\varphi}(x,t)\,dx\,dt$$

$$b:\Phi\times L^2(0,T;H_0^1(0,1))\to\mathbb{R}, \quad b(\varphi,\lambda) = \int_0^T < L\varphi,\lambda >_{H^{-1},H_0^1}\ dt$$

$$l:\Phi\to\mathbb{R}, \quad l(\varphi) = - < \varphi_t(\cdot,0), y_0 >_{H^{-1}(0,1),H_0^1(0,1)} + \int_0^1 \varphi(\cdot,0)\, y_1\,dx.$$

In the remaining part of this section we assume that ω, T and the wave operator L are such that the following holds : there exists a constant C_0 (depending on ω, T and the wave operator L) such that

$$\|\varphi(\cdot,0),\varphi_t(\cdot,0)\|^2_{L^2\times H^{-1}} \le C_0\left(\|L\varphi\|^2_{L^2(0,T;H^{-1}(0,1))} + \|\varphi\|^2_{L^2(q_T)}\right), \quad \forall\varphi\in\Phi. \tag{36}$$

This estimate can be proved using Carleman estimates (see [25, 34]) or by the means of multipliers method (see [23]). We refer to [7] for a proof in the more general case where the subset ω depends on the time variable. Inequality (36) is the main ingredient to prove an equivalent result to Theorem 2.1 in the case of distributed control.

THEOREM 3.1 *(i) The mixed formulation* (35) *is well-posed.*

(ii) The unique solution $(\varphi, \lambda) \in \Phi \times L^2(0,T;H^{-1}(0,1))$ *is the unique saddle-point of the Lagrangian* $\mathcal{L} : \Phi \times L^2(0,T;H^{-1}(0,1)) \to \mathbb{R}$ *defined by* $\mathcal{L}(\varphi,\lambda) = \frac{1}{2}a(\varphi,\varphi) + b(\varphi,\lambda) - l(\varphi)$.

(iii) The optimal function φ *is the minimizer of* $\hat{J}^\star$*, defined by* (34)*, over* Φ *while the optimal function* $\lambda \in L^2(Q_T)$ *is the state of the controlled wave equation* (1) *in the weak sense.*

Since we assume that (36) holds, the proof of Theorem (3.1) is similar to the one of Theorem 2.1, and all the methodology described in Section 2 applies to approximate the distributed control of minimal $L^2(q_T)$-norm. We omit the details and refer to [7] for a more general situation. Numerical results for the approximation of distributed control of minimal L^2-norm are discussed at the end of Section 4.

Remark 2 *The result of this section remains true if we define the space* W *such that* $L\varphi$ *belongs to* $L^2(Q_T)$*. This allows to avoid scalar product over* H^{-1}*. The estimate (36) still holds and the multiplier* λ *is now only in* $L^2(Q_T)$ *and is a controlled solution of (33) in the sense of the transposition. As for the boundary situation, we may also work with* $(\varphi(\cdot,0);\varphi_t(\cdot,0))$ *in* $H_0^1(0,1) \times L^2(0,1)$ *leading naturally to* $L\varphi = 0$ *as an* $L^2(Q_T)$ *function: however, the controls we then get are only in* $H^{-1}(q_T)$ *(see [27, Chapter 7, Section 2]).*

4 Numerical approximation and experiments

4.1 Discretization

We now turn to the discretization of the mixed formulation (20) assuming $r > 0$.

Let then Φ_h and M_h be two finite dimensional spaces parametrized by the variable h such that

$$\Phi_h \subset \Phi, \quad M_h \subset L^2(Q_T), \quad \forall h > 0.$$

Then, we can introduce the following approximated problems : find $(\varphi_h, \lambda_h) \in \Phi_h \times M_h$ solution of

$$\left\{ \begin{array}{rcll} a_r(\varphi_h, \overline{\varphi}_h) + b(\overline{\varphi}_h, \lambda_h) & = & l(\overline{\varphi}_h), & \forall \overline{\varphi}_h \in \Phi_h \\ b(\varphi_h, \overline{\lambda}_h) & = & 0, & \forall \overline{\lambda}_h \in M_h. \end{array} \right. \tag{37}$$

The well-posedness of this mixed formulation is again a consequence of two properties : the coercivity of the bilinear form a_r on the subset $\mathcal{N}_h(b) = \{\varphi_h \in \Phi_h; b(\varphi_h, \lambda_h) = 0 \quad \forall \lambda_h \in M_h\}$. Actually, from the relation

$$a_r(\varphi,\varphi) \geq \frac{r}{\eta}\|\varphi\|_\Phi^2, \quad \forall \varphi \in \Phi$$

the form a_r is coercive on the full space Φ, and so *a fortiori* on $\mathcal{N}_h(b) \subset \Phi_h \subset \Phi$. The second property is a discrete inf-sup condition : there exists $\delta_h > 0$ such that

$$\inf_{\lambda_h \in M_h} \sup_{\varphi_h \in \Phi_h} \frac{b(\varphi_h, \lambda_h)}{\|\varphi_h\|_{\Phi_h}\|\lambda_h\|_{M_h}} \geq \delta_h. \tag{38}$$

For any fixed h, the spaces M_h and Φ_h are of finite dimension so that the infimum and supremum in (38) are reached: moreover, from the property of the bilinear form a_r, it is standard to prove that δ_h is strictly positive (see Section 4.2). Consequently, for any fixed $h > 0$, there exists a unique couple (φ_h, λ_h) solution of (37). On the other hand, the property $\inf_h \delta_h > 0$ is in general difficult to prove and depends strongly on the choice made for the approximated spaces M_h and Φ_h. We shall analyze numerically this property in Section 4.2.

As in [11], the finite dimensional and conformal space Φ_h must be chosen such that $L\varphi_h$ belongs to $L^2(Q_T)$ for any $\varphi_h \in \Phi_h$. This is guaranteed as soon as φ_h possesses second-order derivatives in

$L^2_{loc}(Q_T)$. Therefore, a conformal approximation based on standard triangulation of Q_T requires spaces of functions continuously differentiable with respect to both variables x and t.

We introduce a triangulation $\mathcal{T}_h$ such that $\overline{Q_T} = \cup_{K\in\mathcal{T}_h} K$ and we assume that $\{\mathcal{T}_h\}_{h>0}$ is a regular family. Then, we introduce the space Φ_h as follows :

$$\Phi_h = \{\varphi_h \in C^1(\overline{Q_T}) : \varphi_h|_K \in \mathbb{P}(K) \quad \forall K \in \mathcal{T}_h,\ \varphi_h = 0 \text{ on } \Sigma_T\}$$

where $\mathbb{P}(K)$ denotes an appropriate space of polynomial functions in x and t. In this work, we consider the following two choices for $\mathbb{P}(K)$:

(i) The *Bogner-Fox-Schmit* (BFS for short) C^1 element defined for rectangles. It involves 16 degrees of freedom, namely the values of $\varphi_h, \varphi_{h,x}, \varphi_{h,t}, \varphi_{h,xt}$ on the four vertices of each rectangle K. Therefore $\mathbb{P}(K) = \mathbb{P}_{3,x} \otimes \mathbb{P}_{3,t}$ where $\mathbb{P}_{r,\xi}$ is by definition the space of polynomial functions of order r in the variable ξ. We refer to [10] page 76;

(ii) The reduced *Hsieh-Clough-Tocher* (HCT for short) C^1 element defined for triangles. This is a so-called composite finite element and involves 9 degrees of freedom, namely the values of $\varphi_h, \varphi_{h,x}, \varphi_{h,t}$ on the three vertices of each triangle K. We refer to [10] page 356 and to [3, 29] where the implementation is discussed.

We also define the finite dimensional space

$$M_h = \{\lambda_h \in C^0(\overline{Q_T}) : \lambda_h|_K \in \mathbb{Q}(K) \quad \forall K \in \mathcal{T}_h\},$$

where $\mathbb{Q}(K)$ denotes the space of affine functions both in x and t on the element K. For any $h > 0$, we have $\Phi_h \subset \Phi$ and $M_h \subset L^2(Q_T)$.

Let $n_h = \dim \Phi_h, m_h = \dim M_h$ and let the real matrices $A_{r,h} \in \mathbb{R}^{n_h,n_h}$, $B_h \in \mathbb{R}^{m_h,n_h}$, $J_h \in \mathbb{R}^{m_h,m_h}$ and $L_h \in \mathbb{R}^{n_h}$ be defined by

$$\begin{cases} a_r(\varphi_h, \overline{\varphi_h}) =< A_{r,h}\{\varphi_h\}, \{\overline{\varphi_h}\} >_{\mathbb{R}^{n_h},\mathbb{R}^{n_h}}, \quad \forall \varphi_h, \overline{\varphi_h} \in \Phi_h, \\ b(\varphi_h, \lambda_h) =< B_h\{\varphi_h\}, \{\lambda_h\} >_{\mathbb{R}^{m_h},\mathbb{R}^{m_h}}, \quad \forall \varphi_h \in \Phi_h, \forall \lambda_h \in M_h, \\ \displaystyle\iint_{Q_T} \lambda_h \overline{\lambda_h}\, dx\, dt =< J_h\{\lambda_h\}, \{\overline{\lambda_h}\} >_{\mathbb{R}^{m_h},\mathbb{R}^{m_h}}, \quad \forall \lambda_h, \overline{\lambda_h} \in M_h, \\ l(\varphi_h) =< L_h, \{\varphi_h\} >, \quad \forall \varphi_h \in \Phi_h \end{cases}$$

where $\{\varphi_h\} \in \mathbb{R}^{n_h,1}$ denotes the vector associated to φ_h and $< \cdot,\cdot >_{\mathbb{R}^{n_h},\mathbb{R}^{n_h}}$ the usual scalar product over $\mathbb{R}^{n_h}$. With these notations, the problem (37) reads as follows : find $\{\varphi_h\} \in \mathbb{R}^{n_h}$ and $\{\lambda_h\} \in \mathbb{R}^{m_h}$ such that

$$\begin{pmatrix} A_{r,h} & B_h^T \\ B_h & 0 \end{pmatrix}_{\mathbb{R}^{n_h+m_h,n_h+m_h}} \begin{pmatrix} \{\varphi_h\} \\ \{\lambda_h\} \end{pmatrix}_{\mathbb{R}^{n_h+m_h}} = \begin{pmatrix} L_h \\ 0 \end{pmatrix}_{\mathbb{R}^{n_h+m_h}}. \tag{39}$$

The matrix $A_{r,h}$ as well as the mass matrix J_h are symmetric and positive definite for any $h > 0$ and any $r > 0$. On the other hand, the matrix of order $m_h + n_h$ in (39) is symmetric but not positive definite. We use exact integration methods developed in [14] for the evaluation of the coefficients of the matrices. The system (39) is solved using the direct LU decomposition method.

Let us also mention that for $r = 0$, althought the formulation (20) is well-posed, numerically, the corresponding matrix $A_{0,h}$ is not invertible. In the sequel, we shall consider strictly positive values for r.

Once an approximation φ_h is obtained, the relation (17) leads to an approximation v_h of the control v: precisely, we define

$$v_h = c(1)\pi_{\Delta t}(\varphi_{h,x}(1,\cdot)) \quad \text{in} \quad (0,T) \tag{40}$$

where $\pi_{\Delta t}$ denotes the projection operator on the space of piecewise affine time function: v_h is piecewise linear and coincides at each node (of the mesh $\mathcal{T}_h$) that belongs to the boundary $\{1\} \times (0,T)$, with $c(1)\varphi_{h,x}(1,\cdot)$. Note that in view of the definition of the space Φ_h, the derivative with respect to x of φ_h is a degree of freedom of $\{\varphi_h\}$: hence, the computation of v_h does not require any additional calculus. The corresponding controlled state y_h may be obtained by solving (1) with standard forward approximation (we refer to [11], Section 4 where this is detailed). Here, since the controlled state is directly given by the multiplier λ, we simply use λ_h as an approximation of y and we do not report here the computation of y_h.

Let us now comment on the meshes we use in the next section.

For the Bogner-Fox-Schmidt (BFS) finite element, we use uniform rectangular meshes. Each element is a rectangle of lengths Δx and Δt; $\Delta x > 0$ and $\Delta t > 0$ denote as usual the discretization parameters in space and time respectively. In the numerical experiments, we shall consider five levels of meshes , that is we consider $(\Delta x, \Delta t) = (1/N, 1/N)$ for $N = 10, 20, 40, 80$ and $N = 160$.

For the Hsieh-Clough-Tocher (HCT), we use two types of meshes :

- Uniform triangular meshes obtained from the previous one by dividing each rectangle into two: thus, all the elements are rectangular triangles of the same shape and size, determined by Δx and Δt.
- Non uniform but regular triangular meshes obtained by Delaunay triangulation. Each triangle of the mesh touching the boundaries $(0,1) \times \{0,T\}$ has the side on the boundary of length Δx; similarly, each triangle touching the boundaries $\{0,1\} \times (0,T)$ has the side on that boundary of length Δt.

Again, for the HCT element, we shall consider five levels of meshes: $(\Delta x, \Delta t) = (1/N, T/(2N))$ for $N = 10, 20, 40, 80$ and $N = 160$. As an example, Figure 1 displays uniform rectangular, uniform and non-uniform triangular meshes of Q_T for $N = 10$ and $T = 2$.

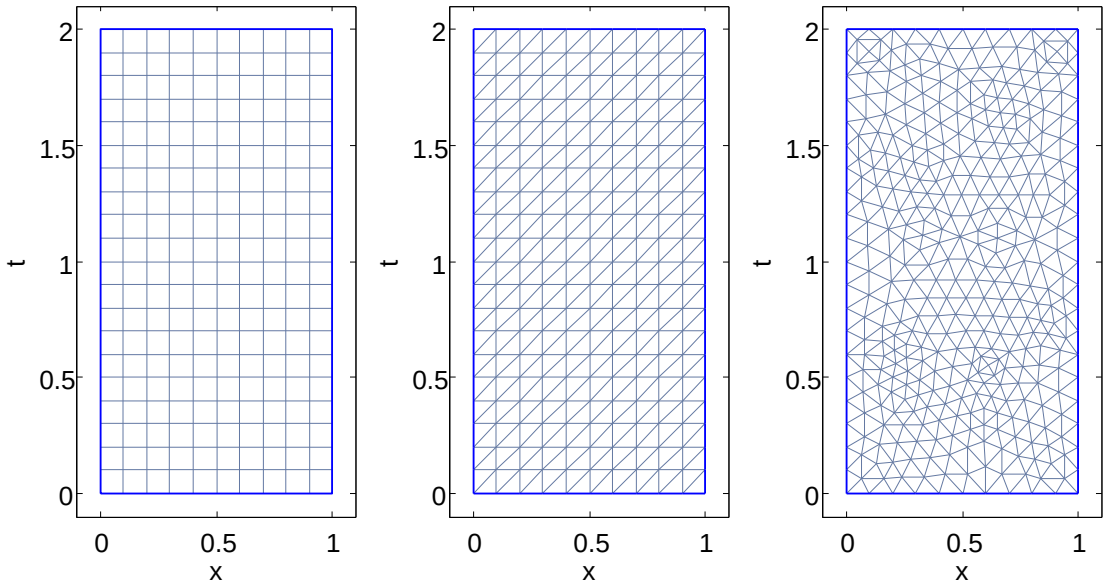

Figure 1: Meshes for $N = 10$. From left to right : a rectangular mesh used for BFS, a triangular uniform mesh and a triangular non-uniform mesh used for HCT.

We note

$$h := \max\{\mathrm{diam}(K), K \in \mathcal{T}_h\}$$

where diam(K) denotes the diameter of K ; the parameter h decreases as the parameter N, defining the fineness of the mesh, increases. Table 1 reports for $T = 2$ the corresponding number of elements and nodes with respect to N.

N	10	20	40	80	160
card$(\mathcal{T}_h)$ - BFS	200	800	3 200	12 800	51 200
card $(\mathcal{T}_h)$ - HCT uniform	400	1 600	6 400	25 600	102 400
card$(\mathcal{T}_h)$ - HCT non uniform	568	2 272	9 088	36 452	145 408
♯ nodes -BFS/HCT uniform	231	861	3 321	13 041	56 681
♯ nodes -HCT non uniform	688	2 752	11 008	44 032	176 128
h - BFS/HCT uniform	1.41×10^{-1}	7.01×10^{-2}	3.53×10^{-2}	1.76×10^{-2}	8.83×10^{-3}
h - HCT non uniform	9.02×10^{-2}	4.51×10^{-2}	2.55×10^{-2}	1.13×10^{-2}	5.6×10^{-3}

Table 1: Number of elements (rectangle for BFS and triangle for HCT), number of nodes and value of h for each type of meshes w.r.t. to the integer N - $T = 2$.

4.2 The discrete inf-sup test

Before to give and discuss some numerical experiments, we first test numerically the discrete inf-sup condition (38). Taking $\eta = r > 0$ so that $a_r(\varphi, \overline{\varphi}) = (\varphi, \overline{\varphi})_\Phi$ exactly for all $\varphi, \overline{\varphi} \in \Phi$, it is readily seen (see for instance [9]) that the discrete inf-sup constant satisfies

$$\delta_h = \inf\Big\{ \sqrt{\delta} : B_h A_{r,h}^{-1} B_h^T \{\lambda_h\} = \delta\, J_h\{\lambda_h\}, \quad \forall\, \{\lambda_h\} \in \mathbb{R}^{m_h} \setminus \{0\} \Big\}. \tag{41}$$

The matrix $B_h A_{r,h}^{-1} B_h^T$ enjoys the same properties than the matrix $A_{r,h}$: it is symmetric and positive definite so that the scalar δ_h defined in term of the (generalized) eigenvalue problem (41) is strictly positive. This eigenvalue problem is solved using the power iteration algorithm (assuming that the lowest eigenvalue is simple): for any $\{v_h^0\} \in \mathbb{R}^{n_h}$ such that $\|\{v_h^0\}\|_2 = 1$, compute for any $n \geq 0$, $\{\varphi_h^n\} \in \mathbb{R}^{n_h}, \{\lambda_h^n\} \in \mathbb{R}^{m_h}$ and $\{v_h^{n+1}\} \in \mathbb{R}^{m_h}$ iteratively as follows :

$$\begin{cases} A_{r,h}\{\varphi_h^n\} + B_h^T\{\lambda_h^n\} = 0 \\ B_h\{\varphi_h^n\} = -J_h\{v_h^n\} \end{cases}, \quad \{v_h^{n+1}\} = \frac{\{\lambda_h^n\}}{\|\{\lambda_h^n\}\|_2}.$$

The scalar δ_h defined by (41) is then given by : $\delta_h = \lim_{n\to\infty}(\|\{\lambda_h^n\}\|_2)^{-1/2}$.

We now give some numerical values of δ_h with respect to N (equivalently with respect to h) for the two C^1 finite elements introduced in Section 4.1. We take here for simplicity $c := 1$ and $d := 0$ so that $L\,\varphi := \varphi_{tt} - \varphi_{xx}$. Values of c and d do not affect qualitatively the results.

Table 2 is concerned with the BFS element and $T = 2$. Table 3 is concerned with the HCT element for uniform meshes. Table 4 is concerned with the HCT element for non uniform meshes.

As expected, we check that δ_h decreases as $h \to 0$ and increases as $r \to 0$. More importantly, we observe that for any r, the value of δ_h does not seem to be bounded by below with respect to the discretization parameter: for low values of r, the decrease of δ_h as $h \to 0$ seems however very slow (see first row of Table 2 and Figure 2). We recall that the scalars r, η are arbitrary as long as they are strictly positive, so that the form a_r defines a scalar product over Φ. In the first two cases where the meshes are uniform (that is $\Delta t = \Delta x$), it is worth to note that we obtain the same behavior when $\Delta x \neq \Delta t$.

We may conclude that the two finite elements considered here do not "pass" the discrete inf-sup test. As we shall see in the next section, this interesting fact does not prevent the convergence of the sequence φ_h and λ_h, at least for the cases we have considered. Interestingly, we also observe that the discrete inf-sup constant δ_h remains bounded with respect to h when the parameter r depends appropriately on h (last row of Tables 2, 3, 4).

h	1.41×10^{-1}	7.01×10^{-2}	3.53×10^{-2}	1.76×10^{-2}	8.83×10^{-3}
$r = 1$	0.466	0.253	0.123	0.060	0.030
$r = 10^{-2}$	1.474	1.427	1.178	0.599	0.300
$r = 10^{-4}$	3.364	2.247	1.729	1.524	1.451
$r = h^2$	1.474	1.483	1.486	1.489	1.497

Table 2: δ_h w.r.t. r and h - $T = 2$. for the BFS element.

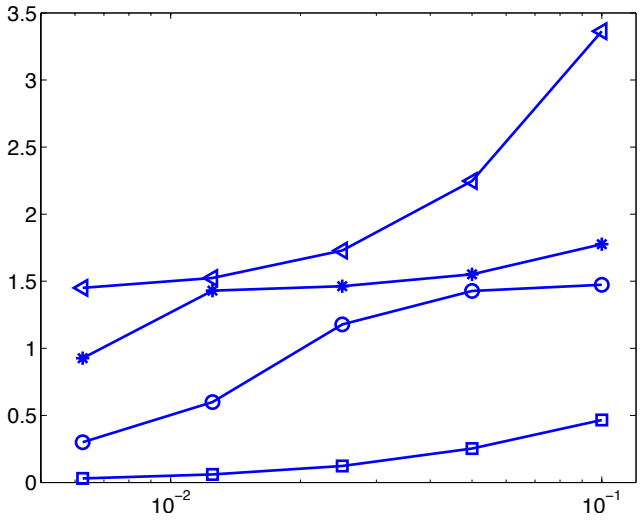

Figure 2: BFS finite element - Evolution of the inf-sup constante δ_h with respect to h (see Table 2) for $r = 10^{-4}$ ($<$), $r = 10^{-3}$ ($\star$), $r = 10^{-2}$ ($\circ$) and $r = 10^{-1}$ ($\square$).

h	1.41×10^{-1}	7.01×10^{-2}	3.53×10^{-2}	1.76×10^{-2}	8.83×10^{-3}
$r = 1$	0.3593	0.2519	0.1782	0.1263	0.0886
$r = 10^{-2}$	1.6626	1.4717	1.4173	1.1939	0.8521
$r = 10^{-4}$	8.7279	4.4403	2.5027	1.74	1.4992
$r = h$	1.0939	1.0791	1.0764	1.0769	1.0438
$r = h^2$	1.6625	1.6532	1.6416	1.6310	1.6214

Table 3: δ_h w.r.t. r and h - $T = 2$. for the HCT element and uniform mesh.

h	9.02×10^{-2}	4.51×10^{-2}	2.55×10^{-2}	1.13×10^{-2}	5.6×10^{-3}
$r = 1$	0.4029	0.2841	0.1885	0.1211	0.0782
$r = 10^{-2}$	1.623	1.4602	1.4149	1.1925	0.7807
$r = 10^{-4}$	7.9374	4.059	2.3286	1.6749	1.4797
$r = h$	1.2637	1.2424	1.1679	1.0705	0.9805
$r = h^2$	1.623	1.6132	1.5998	1.5867	1.5752

Table 4: δ_h w.r.t. r and h - $T = 2$. for the HCT element and non uniform mesh.

4.3 Numerical experiments: the boundary case

We first address the boundary case for three initial data with various regularity and for which we know explicitly the control v of minimal L^2-norm. This allows to evaluate precisely the error $\|v-v_h\|_{L^2(0,T)}$ with respect to h and confirm the relevance of the method. For these three examples, we take $c := 1$ and $d := 0$.

For any $m \in \mathbb{N}$, let us first consider the initial condition

$$(\mathbf{EX1}) \qquad y_0(x) = \sin(m\pi x), \quad y_1(x) = 0, \quad T = 2$$

for which the control of minimal L^2-norm is given by $v(t) = \frac{1}{2}(-1)^{m+1}\sin(m\pi t)$ on $[0,T]$ while the adjoint state $\varphi \in \Phi$, minimizer of the conjugate functional $\hat{J}^\star$ (see (18)) has the expression $\varphi(x,t) = -\frac{1}{2m\pi}\sin(m\pi t)\sin(m\pi x)$ in Q_T. We have $\|v\|_{L^2(0,T)} = 1/2$.

We take $m = 3$. We first give some numerical values obtained with the BFS element. Tables 5 and 6 collect some numerical values for $r = 10^{-2}$ and $r = 1$ respectively. Values corresponding to $r = 10^{-4}, h^2$ and $r = 10^2$ are reported in the Appendix, Table 21, 22, 23.

In the Tables, κ denotes the condition number associated to (39), independent of the initial data (y_0, y_1) [1].

The convergence of $\|\varphi - \varphi_h\|_{L^2(Q_T)}$, $\|v - v_h\|_{L^2(0,T)}$ and $\|L\varphi_h\|_{L^2(Q_T)}$ toward zero as $h \to 0$ is observed. We observe that, as soon as h is small enough, the value of the positive parameter $r > 0$ has a reduced impact on the results.

We observe that a low value of r, for instance $r = 10^{-4}$, (providing a "better" inf-sup constant δ_h) leads to a faster convergence of the Lagrangian variable λ_h than the value $r = 1$. This is in agreement with the classical estimates for mixed finite element approximation. Note that the phenomenon is however restricted here. On the other hand, a larger value of r allows a faster convergence of the dual variable φ_h, since the constraint is better represented (observe the locking phenomenon for $r = 10^{-2}$ when h is large, Table 23). The case $r = h^2$ (Table 22) offers an interesting compromise, although quite large values for $\|L\varphi_h\|_{L^2(Q_T)}$. Moreover, this case provides the lowest values for κ. Finally, in every case, the condition number behaves polynomially with respect to h.

[1] The condition number $\kappa(\mathcal{M}_h)$ of any square matrix $\mathcal{M}_h$ is defined by $\kappa(\mathcal{M}_h) = |||\mathcal{M}_h|||_2 |||\mathcal{M}_h^{-1}|||_2$ where the norm $|||\mathcal{M}_h|||_2$ stands for the largest singular value of $\mathcal{M}_h$.

We compute

$$r = 1: \quad \|\varphi - \varphi_h\|_{L^2(Q_T)} \approx O(h^{3.9}), \quad \|v - v_h\|_{L^2(0,T)} \approx O(h^{3.5}), \quad \|L\varphi_h\|_{L^2(Q_T)} \approx O(h^{1.96}),$$
$$r = 10^{-2}: \quad \|\varphi - \varphi_h\|_{L^2(Q_T)} \approx O(h^{3}), \quad \|v - v_h\|_{L^2(0,T)} \approx O(h^{2.}), \quad \|L\varphi_h\|_{L^2(Q_T)} \approx O(h^{1.92}).$$

h	1.41×10^{-1}	7.01×10^{-2}	3.53×10^{-2}	1.76×10^{-2}	8.83×10^{-3}
$\|\varphi - \varphi_h\|_{L^2(Q_T)}$	2.63×10^{-3}	2.88×10^{-4}	3.68×10^{-5}	4.82×10^{-6}	6.08×10^{-7}
$\|v - v_h\|_{L^2(0,T)}$	5.32×10^{-2}	1.3×10^{-2}	3.29×10^{-3}	8.01×10^{-4}	1.98×10^{-4}
$\|v_h\|_{L^2(0,T)}$	0.499	0.501	0.5	0.5	0.5
$\|L\varphi_h\|_{L^2(Q_T)}$	1.371×10^{0}	2.69×10^{-1}	6.24×10^{-2}	2.05×10^{-2}	6.33×10^{-3}
$\|\lambda_h\|_{L^2(Q_T)}$	0.498	0.499	0.499	0.5	0.5
κ	9.42×10^{7}	9.67×10^{8}	1.97×10^{10}	4.63×10^{11}	1.08×10^{13}

Table 5: Example **EX1** - BFS element - $r = 10^{-2}$.

h	1.41×10^{-1}	7.01×10^{-2}	3.53×10^{-2}	1.76×10^{-2}	8.83×10^{-3}
$\|\varphi - \varphi_h\|_{L^2(Q_T)}$	2.68×10^{-3}	2.13×10^{-4}	1.39×10^{-5}	8.81×10^{-7}	5.53×10^{-8}
$\|v - v_h\|_{L^2(Q_T)}$	3.87×10^{-2}	2.92×10^{-3}	1.95×10^{-4}	1.68×10^{-5}	2.75×10^{-6}
$\|v_h\|_{L^2(0,T)}$	0.457	0.496	0.4998	0.4999	0.5
$\|L\varphi_h\|_{L^2(Q_T)}$	1.38×10^{-1}	3.8×10^{-2}	9.7×10^{-3}	2.44×10^{-3}	6.14×10^{-4}
$\|\lambda_h\|_{L^2(Q_T)}$	0.484	0.498	0.4999	0.4999	0.5
κ	1.52×10^{8}	4.42×10^{9}	1.19×10^{11}	7.33×10^{12}	4.55×10^{14}

Table 6: Example **EX1** - BFS element - $r = 1$.

Tables 7 and 8 report the result obtained for the HCT element on uniform meshes for $r = 1$ and $r = 10^{-2}$ respectively. For this element, we observe that the value of r has a deeper impact on the quality of the result. The convergence observed for $r = 10$ w.r.t. h is very slow (see Table 24 in the appendix). A better convergence is observed for lower values ($r = 1, 10^{-2}$ and lower). We compute that :

$$r = 1: \quad \|\varphi - \varphi_h\|_{L^2(Q_T)} \approx O(h^{1.13}), \quad \|v - v_h\|_{L^2(0,T)} \approx O(h^{1.15})$$
$$r = 10^{-2}: \quad \|\varphi - \varphi_h\|_{L^2(Q_T)} \approx O(h^{2.21}), \quad \|v - v_h\|_{L^2(0,T)} \approx O(h^{2.08}).$$

The rates of convergence for the HCT element-uniform mesh are significantly reduced with respect to the rates obtained for the BFS element: as a possible explanation, we emphasize that the BFS element is slightly richer since he contains in addition the cross derivative $\varphi_{h,xt}$ as degree of freedom. We also observe that the influence of the parameter r is even more important for non uniform mesh when the HCT element is used (see Tables 27, 28), so that this element seems more sensitive to the lack of uniform inf-sup property discussed in Section 4.2. In this respect, when r behaves like h^2, we observe in both cases a very good convergence of the variable φ_h and λ_h together with a significant reduction of the condition number κ (see Table 25). Again, this condition number increases polynomially as h goes to 0. We recall that the condition number of the discrete HUM operator blows up exponentially w.r.t. h when a non uniformly controllable approximation is used (see [30]).

The second initial data corresponds to a continuous but not $C^1(0,1)$ initial position :

$$(\mathbf{EX2}) \qquad y_0(x) = 16x^3\, 1_{(0,1/2)}(x) + 16(1-x)^3\, 1_{(1/2,1)}(x), \quad y_1(x) = 0, \quad T = 2$$

for which the control of minimal L^2-norm is given by

$$v(t) = 8t^3\, 1_{(0,1/2)}(t) + 8(1-t)^3\, 1_{(1/2,3/2)}(t) - 8(2-t)^3\, 1_{(3/2,2)}(t), \quad t \in (0,T)$$

h	1.41×10^{-1}	7.01×10^{-2}	3.53×10^{-2}	1.76×10^{-2}	8.83×10^{-3}
$\|\varphi-\varphi_h\|_{L^2(Q_T)}$	2.71×10^{-2}	1.99×10^{-2}	8.75×10^{-3}	2.6×10^{-3}	7.08×10^{-4}
$\|v-v_h\|_{L^2(0,T)}$	3.79×10^{-1}	2.66×10^{-1}	1.1×10^{-1}	3.5×10^{-2}	9.3×10^{-3}
$\|v_h\|_{L^2(0,T)}$	0.08	0.2239	0.3822	0.4642	0.4905
$\|L\varphi_h\|_{L^2(Q_T)}$	1.87×10^{-1}	2.4×10^{-1}	2.1×10^{-1}	1.28×10^{-1}	6.8×10^{-2}
$\|\lambda_h\|_{L^2(Q_T)}$	0.4368	0.4392	0.4658	0.4885	0.4968
κ	2.24×10^{8}	5.05×10^{9}	1.4×10^{11}	5.88×10^{12}	5.57×10^{16}

Table 7: Example **EX1** - HCT element - Uniform mesh - $r=1$.

h	1.41×10^{-1}	7.01×10^{-2}	3.53×10^{-2}	1.76×10^{-2}	8.83×10^{-3}
$\|\varphi-\varphi_h\|_{L^2(Q_T)}$	3.69×10^{-3}	4.81×10^{-4}	1.13×10^{-4}	2.85×10^{-5}	7.17×10^{-6}
$\|v-v_h\|_{L^2(0,T)}$	5.26×10^{-2}	1.21×10^{-2}	3.02×10^{-3}	7.19×10^{-4}	1.61×10^{-4}
$\|v_h\|_{L^2(0,T)}$	0.4773	0.4939	0.4984	0.4996	0.4999
$\|L\varphi_h\|_{L^2(Q_T)}$	1.7803	6.16×10^{-1}	2.85×10^{-1}	1.4×10^{-1}	6.96×10^{-2}
$\|\lambda_h\|_{L^2(Q_T)}$	0.4938	0.4986	0.4997	0.4999	0.5
κ	2.85×10^{5}	2.53×10^{6}	3.66×10^{7}	6.19×10^{8}	3.03×10^{10}

Table 8: Example **EX1** - HCT element - Uniform mesh - $r=10^{-2}$.

leading to $\|v\|_{L^2(0,T)}=\sqrt{14}/7\approx 0.53452$.

Tables 9 and 10 collect some values for $r=1$ and $r=10^{-2}$ respectively when the BFS finite element is used. Again, the influence of the value of r is weak. For this set of data, less regular than the previous one, we observe a lower rate of convergence with respect to h :

$$r=1: \quad \|v-v_h\|_{L^2(0,T)}\approx e^{-0.71}h^{0.93}, \quad \|L\varphi_h\|_{L^2(Q_T)}\approx e^{-0.54}h^{0.96},$$
$$r=10^{-2}: \quad \|v-v_h\|_{L^2(0,T)}\approx e^{-1.28}h^{0.78}, \quad \|L\varphi_h\|_{L^2(Q_T)}\approx e^{3.66}h^{1.56}.$$

h	1.41×10^{-1}	7.01×10^{-2}	3.53×10^{-2}	1.76×10^{-2}	8.83×10^{-3}
$\|v_h\|_{L^2(0,T)}$	0.5291	0.5325	0.5339	0.5343	0.5344
$\|v-v_h\|_{L^2(0,T)}$	7.62×10^{-2}	4.19×10^{-2}	2.20×10^{-2}	1.13×10^{-2}	5.76×10^{-3}
$\|\lambda_h\|_{L^2(Q_T)}$	0.541	0.536	0.5349	0.5346	0.5345
$\|L\varphi_h\|_{L^2(Q_T)}$	8.53×10^{-2}	4.52×10^{-2}	2.31×10^{-2}	1.17×10^{-2}	5.88×10^{-3}

Table 9: Example **EX2** - BFS element - $r=1$.

Tables 11 and 12 correspond to $r=1$ and $r=10^{-2}$ respectively when the HCT element with non uniform meshes is used. We obtain again a slightly lower rate of convergence :

$$r=1: \quad \|v-v_h\|_{L^2(0,T)}\approx e^{0.01}h^{0.71}, \quad \|L\varphi_h\|_{L^2(Q_T)}\approx e^{-0.32}h^{0.56},$$
$$r=10^{-2}: \quad \|v-v_h\|_{L^2(0,T)}\approx e^{-1.06}h^{0.84}, \quad \|L\varphi_h\|_{L^2(Q_T)}\approx e^{2.97}h^{1.09}.$$

The third example is much stiffer in the sense that the initial position belongs to $L^2(0,1)$ but is discontinuous:

$$(\mathbf{EX3}) \qquad y_0(x)=4x\,1_{(0,1/2)}(x), \quad y_1(x)=0, \quad T=2.4.$$

The corresponding control of minimal L^2-norm, discontinuous, is given by $v(t)=2(1-t)\,1_{(1/2,3/2)}(t)$, $t\in(0,T)$ so that $\|v\|_{L^2(0,T)}=1/\sqrt{3}\approx 0.5773$. When the classical dual method (that is, the minimization of a discrete conjugate functional with respect to the initial data of the adjoint solution) is employed, adapted schemes are needed to obtain convergent results (we refer to [30] and the references therein).

h	1.41×10^{-1}	7.01×10^{-2}	3.53×10^{-2}	1.76×10^{-2}	8.83×10^{-3}
$\|v_h\|_{L^2(0,T)}$	0.5467	0.5375	0.5352	0.5347	0.5345
$\|v - v_h\|_{L^2(0,T)}$	4.34×10^{-2}	2.06×10^{-2}	9.47×10^{-3}	4.3×10^{-3}	2.02×10^{-3}
$\|\lambda_h\|_{L^2(Q_T)}$	0.5469	0.5377	0.5353	0.5347	0.5346
$\|L\varphi_h\|_{L^2(Q_T)}$	1.85×10^{0}	6.18×10^{-1}	2.01×10^{-1}	6.7×10^{-2}	2.49×10^{-2}

Table 10: Example **EX2** - BFS element - $r = 10^{-2}$.

h	9.02×10^{-2}	4.51×10^{-2}	2.55×10^{-2}	1.13×10^{-2}	5.6×10^{-3}
$\|v_h\|_{L^2(0,T)}$	0.4794	0.4976	0.5167	0.5268	0.5313
$\|v - v_h\|_{L^2(0,T)}$	1.86×10^{-1}	1.15×10^{-1}	7.1×10^{-2}	4.29×10^{-2}	2.57×10^{-2}
$\|\lambda_h\|_{L^2(Q_T)}$	0.5461	0.5336	0.5327	0.5334	0.534
$\|L\varphi_h\|_{L^2(Q_T)}$	1.49×10^{-1}	1.25×10^{-1}	8.81×10^{-2}	5.84×10^{-2}	3.75×10^{-2}

Table 11: Example **EX2** - HCT element - Non uniform mesh - $r = 1$.

Table 13 collects some values for $r = 1$ when the BFS finite element is used (the case $r = 10^{-2}$ gives very closed results and is reported in Table 31, see the appendix). We observe the following rate of convergence with respect to h :

$$r = 1 : \quad \|v - v_h\|_{L^2(0,T)} \approx e^{-0.37} h^{0.45}, \quad \|L\varphi_h\|_{L^2(Q_T)} \approx e^{-1.57} h^{0.37},$$
$$r = 10^{-2} : \quad \|v - v_h\|_{L^2(0,T)} \approx e^{-0.09} h^{0.52}, \quad \|L\varphi_h\|_{L^2(Q_T)} \approx e^{2.46} h^{0.72}.$$

It is interesting to note, as in the previous examples, that a rather good approximation v_h of the control is obtained with a quite large value of the L^2-norm of $L\varphi_h$. Table 13 also indicates that the $H^{-1}(Q_T)$-norm of $L\varphi_h$ is almost zero. This is due to the fact that the variable $\varphi_h \in \Phi_h$ satisfies $b(\varphi_h, \lambda_h) = 0$ for all $\lambda_h \in M_h$, that M_h is also a conformal approximation of $H^1(0,1)$ and that $\|L\varphi_h\|_{H^{-1}(0,1)} = \sup_{l \in H^1(0,1), \|l\|_{H^1}=1} |b(\varphi_h, l)|$. For any h and any r, the adjoint variable φ_h satisfies the wave equation in a weak sense. This phenomenon is highlighted in Table 14: small values of r (for instance $r = 10^{-6}$, h being fixed) leads to large values of $\|L\varphi_h\|_{L^2(0,1)}$ but to good approximations λ_h and v_h of the controlled solution and of the control respectively.

Tables 15 and 16 provide the results for $r = 1$ obtained with the reduced HCT for uniform and non-uniform meshes respectively :

$$r = 1 - \text{HCT uniform mesh} : \quad \|v - v_h\|_{L^2(0,T)} \approx e^{-0.86} h^{0.22}, \quad \|L\varphi_h\|_{L^2(Q_T)} \approx e^{-0.91} h^{0.32},$$
$$r = 1 - \text{HCT non uniform mesh} : \quad \|v - v_h\|_{L^2(0,T)} \approx e^{-1.03} h^{0.25}, \quad \|L\varphi_h\|_{L^2(Q_T)} \approx e^{-0.55} h^{0.46}.$$

Figure 3 depicts the evolution of the error $\|v - v_h\|_{L^2(0,T)}$ w.r.t. h for the BFS and HCT element. Closed results are observed for $r = 10^{-2}$, reported Tables 32 and 33 in the appendix.

Figure 4 depicts the corresponding approximation v_h of the HUM control on $(0,T)$ and confirm the remarkable approximation we get in this stiff case. Figures 5 and 6 depict the variable $\varphi_h \subset \Phi_h$ and the multiplier $\lambda_h \subset M_h$ in Q_T respectively. These figures are obtained with a mesh $\mathcal{T}_h$ composed of 9 088 triangles and for which $h = 2.46 \times 10^{-2}$. In agreement with Theorem 2.1, item (iii), λ_h is an approximation of the controlled solution for (1). We have used here $r = 10^{-2}$.

We also emphasize that this variational method which requires a finite element discretization of the time-space Q_T is particularly well-adapted to mesh optimization. Still for the example **EX3**, Figure 7 depicts a sequence of five distinct meshes of $Q_T = (0,1) \times (0,T)$: the sequence is initiated with a coarse and regularly distributed mesh, corresponding to $N = 5$. The four other meshes are successively obtained by local refinement based on the norm of the gradient of λ_h on each triangle of $\mathcal{T}_h$. As expected, the refinement is concentrated around the lines of discontinuity of λ_h (see Figure 9) traveling in Q_T, generated by the discontinuity of the initial position y_0. The five meshes

h	9.02×10^{-2}	4.51×10^{-2}	2.55×10^{-2}	1.13×10^{-2}	5.6×10^{-3}
$\|v_h\|_{L^2(0,T)}$	0.5543	0.5395	0.5356	0.5347	0.5345
$\|v - v_h\|_{L^2(0,T)}$	4.78×10^{-2}	2.56×10^{-2}	1.32×10^{-2}	7.69×10^{-3}	4.56×10^{-3}
$\|\lambda_h\|_{L^2(Q_T)}$	0.5607	0.5417	0.5364	0.535	0.5346
$\|L\varphi_h\|_{L^2(Q_T)}$	1.6996	6.22×10^{-1}	2.63×10^{-1}	1.36×10^{-1}	7.81×10^{-2}

Table 12: Example **EX2** - HCT element - Non uniform mesh - $r = 10^{-2}$.

h	1.41×10^{-1}	7.01×10^{-2}	3.53×10^{-2}	1.76×10^{-2}	8.83×10^{-3}
$\|v_h\|_{L^2(0,T)}$	0.6003	0.5850	0.5776	0.5752	0.5747
$\|v - v_h\|_{L^2(0,T)}$	2.87×10^{-1}	2.05×10^{-1}	1.47×10^{-1}	1.08×10^{-1}	8.18×10^{-2}
$\|\lambda_h\|_{L^2(Q_T)}$	0.62	0.598	0.586	0.581	0.578
$\|L\varphi_h\|_{L^2(Q_T)}$	1.02×10^{-1}	7.53×10^{-2}	5.8×10^{-2}	4.55×10^{-2}	3.6×10^{-2}
$\|L\varphi_h\|_{H^{-1}(Q_T)}$	1.92×10^{-16}	3.83×10^{-16}	7.46×10^{-16}	1.51×10^{-15}	2.81×10^{-15}

Table 13: Example **EX3** - BFS element - $r = 1$.

r	10^{-6}	10^{-4}	10^{-2}	1	10
κ	4.52×10^{12}	3.71×10^{11}	6.05×10^{11}	7.38×10^{12}	7.26×10^{14}
$\|v_h\|_{L^2(0,T)}$	0.5829	2.5827	0.5816	0.5752	0.569
$\|\lambda_h(1,\cdot)\|_{L^2(0,T)}$	0.5848	2.5848	0.5831	0.5759	0.5696
$\|v - v_h\|_{L^2(0,T)}$	1.116×10^{-1}	1.114×10^{-1}	1.079×10^{-1}	1.087×10^{-1}	1.211×10^{-1}
$\|L\varphi_h\|_{L^2(Q_T)}$	5.6×10^{3}	5.6×10^{1}	6.13×10^{-1}	4.56×10^{-2}	1.75×10^{-2}
$\|L\varphi_h\|_{H^{-1}(Q_T)}$	6.85×10^{-14}	5.88×10^{-15}	6.17×10^{-15}	6.06×10^{-15}	6.33×10^{-15}

Table 14: Example **EX3** - BFS element - $h = 1.76 \times 10^{-2}$.

h	1.56×10^{-1}	7.81×10^{-2}	3.90×10^{-2}	1.95×10^{-2}	9.76×10^{-3}
$\|v_h\|_{L^2(0,T)}$	0.4571	0.4923	0.5194	0.5354	0.5467
$\|v - v_h\|_{L^2(Q_T)}$	2.78×10^{-1}	2.3×10^{-1}	2.01×10^{-1}	1.72×10^{-1}	1.47×10^{-1}
$\|\lambda_h\|_{L^2(Q_T)}$	0.5987	0.5799	0.5744	0.5727	0.5728
$\|L\varphi_h\|_{L^2(Q_T)}$	2.2×10^{-1}	1.8×10^{-1}	1.37×10^{-1}	1.11×10^{-1}	9.07×10^{-2}

Table 15: Example **EX3** - HCT element - Uniform mesh - $r = 1$.

h	9.87×10^{-2}	4.93×10^{-2}	2.46×10^{-2}	1.23×10^{-2}	6.17×10^{-3}
$\|v_h\|_{L^2(0,T)}$	0.5191	0.5359	0.5451	0.5523	0.5582
$\|v - v_h\|_{L^2(0,T)}$	2.35×10^{-1}	1.92×10^{-1}	1.61×10^{-1}	1.4×10^{-1}	1.19×10^{-1}
$\|\lambda_h\|_{L^2(Q_T)}$	0.5979	0.5809	0.5748	0.5729	0.5728
$\|L\varphi_h\|_{L^2(Q_T)}$	1.9×10^{-1}	1.42×10^{-1}	1.12×10^{-1}	9.07×10^{-2}	7.5×10^{-2}

Table 16: Example **EX3** - HCT element - Non uniform mesh - $r = 1$.

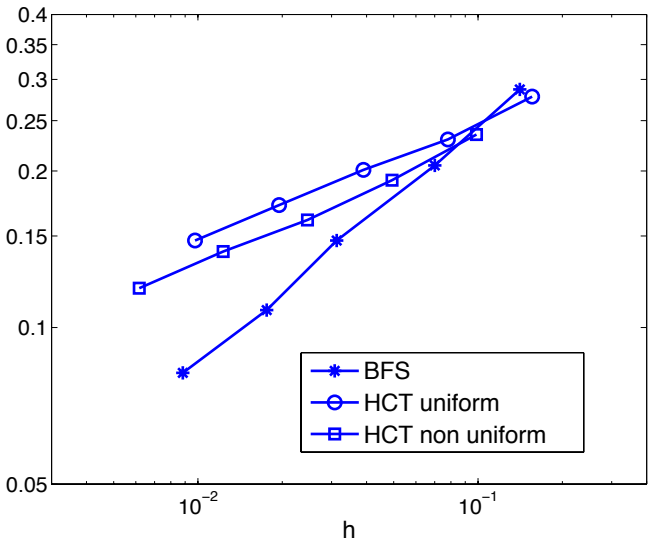

Figure 3: Example **EX3**; Evolution of $\|v - v_h\|_{L^2(0,T)}$ w.r.t. h for BFS finite element ($\star$), HCT-uniform mesh ($\circ$) and HCT- non uniform mesh ($\square$); $r = 1$.

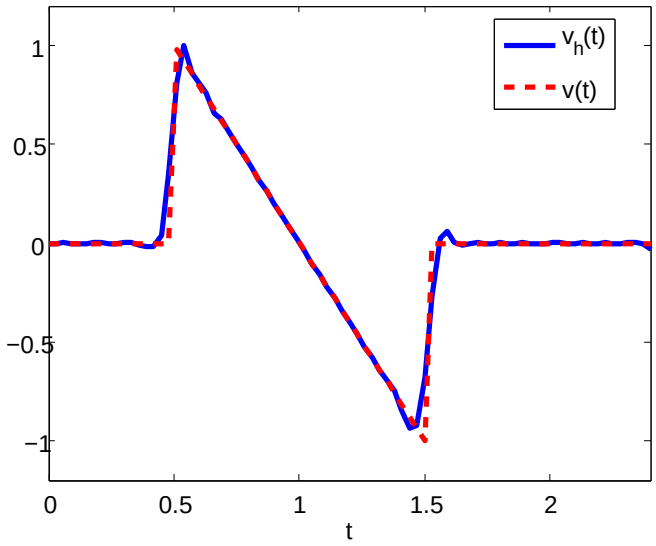

Figure 4: Control of minimal L^2-norm v and its approximation v_h on $(0, T)$.

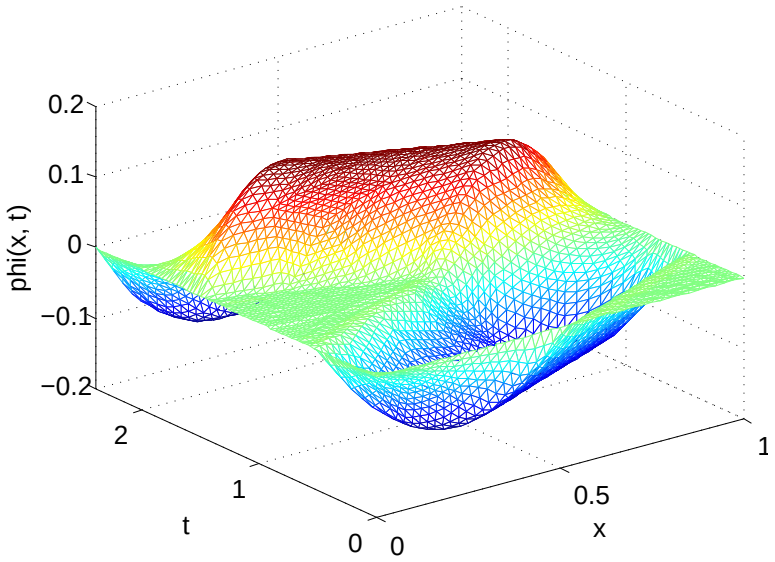

Figure 5: Example **EX3** : The dual variable φ_h in Q_T; $h = 2.46 \times 10^{-2}$; $r = 10^{-2}$.

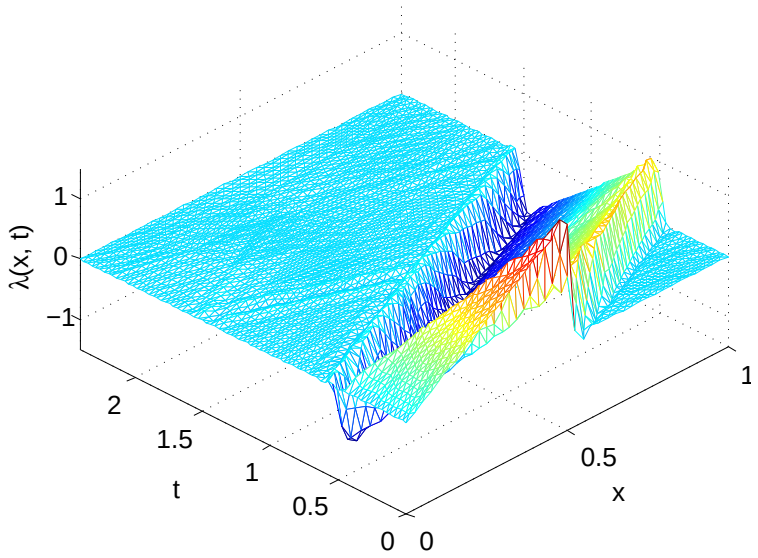

Figure 6: Example **EX3** : The primal variable λ_h in Q_T; $h = 2.46 \times 10^{-2}$; $r = 10^{-2}$.

contain 142, 412, 1 154, 2 556 and 4 750 triangles respectively. The number of nodes in these five meshes is 87, 231, 614, 1 324 and 2 429 respectively. The errors $\|v - v_h\|_{L^2(0,T)}$ corresponding to each of the five meshes (sorted by number of triangles) are : 2.67×10^{-1}, 2.51×10^{-1}, 1.31×10^{-1}, 8.36×10^{-2} and 8.11×10^{-2} respectively.

As a partial conclusion, this direct method offers very good approximations of the control of minimal square-integrable norm, even in singular situations for which classical methods generally fail. It is important to note that the lack of uniform property we have suspected (for r fixed and large enough) from the experiences reported in Section 4.2 does not seem to have a significant influence on the behavior of the method w.r.t. h. For any $r > 0$, the convergence of the approximation is observed as h tends to 0. An intermediate value of r, around 10^{-2}, offers a good compromise between the convergence of the primal variable λ_h and of the dual one φ_h. In this respect, the parameter r may not be seen as an augmentation parameter for the Lagrangian $\mathcal{L}$, but rather as a regularization parameter for the variable φ_h (this enforces $L\varphi_h \in L^2(Q_T)$ uniformly). This also suggests that the constraint $L\varphi \in L^2(Q_T)$ we have settled in the definition of the space W (see 18) may possibly be weakened.

4.4 Conjugate gradient for $J^{\star\star}$

We illustrate here the Section 2.2: we minimize the functional $J^{\star\star} : L^2(Q_T) \to \mathbb{R}$ with respect to the variable λ. We recall that this minimization corresponds exactly to the resolution of the mixed formulation (20) by an iterative Uzawa type procedure. The conjugate gradient algorithm is given at the end of Section 2.2. In practice, each iteration amounts to solve a linear system involving the matrix $A_{r,h}$ of size $n_h = 4m_h$ (see (39)) which is sparse, symmetric and positive definite. We use the Cholesky method.

We consider the singular situation given by the example **EX3**. We take $\varepsilon = 10^{-10}$ as a stopping threshold for the algorithm (that is the algorithm is stopped as soon as the norm of the residue g^n at the iterate n satisfies $\|g^n\|_{L^2(Q_T)} \leq 10^{-10}\|g^0\|_{L^2(Q_T)}$). The algorithm is initiated with $\lambda^0 = 0$ in Q_T.

We discuss only some results obtained with the BFS finite element (the HCT finite element leads to very similar results) and consider uniform meshes with $\Delta t = 1.2\Delta x$ (in order to emphasize that, in this finite element framework, it is absolutely not necessary to consider $\Delta t \leq \Delta x$ when the velocity c of the waves equals one). Tables 17, 18 and 19 display the result for $r = 10^{-2}, 1$ and $r = 10^2$ respectively. We recall that the norm of the control is $\|v\|_{L^2(0,T)} \approx 0.5773$.

We first check that this iterative method gives exactly the same approximation λ_h than the previous direct method (where (39) is solved directly), since problem (20) coincides with the minimization of $J^{\star\star}$ in the sense given by Proposition 2.2 for $r > 0$. Then, we observe that the number of iterates is sub-linear with respect to h, precisely with respect to the dimension $m_h = card(\{\lambda_h\})$ of the approximated problem. Once again, this is in contrast with the behavior of the conjugate gradient algorithm when this latter is used to minimize $J^\star$ with respect to (φ_0, φ_1) (see [30]). Finally, as for the direct method, the influence of the parameter r remains limited. Since the gradient of $J^{\star\star}$ is given by $\nabla J^{\star\star}(\lambda) = L\varphi_0 - A_r\lambda := L\varphi$, a larger r reduces the number of iterates. From this perspective, r can be seen, here, as an augmentation parameter for the constraint $L\varphi = 0$. On the other hand, a larger r reduces the convergence of the primal variable, that is λ_h, and therefore of the control, defined here as the trace $\lambda_h(1, \cdot)$. For $r = 1$ and the discretization corresponding to $h = 9.99 \times 10^{-3}$ (that is $\Delta x = 6.25 \times 10^{-2}$, $\Delta t = 7.79 \times 10^{-2}$), Figure 10 depicts the evolution of the ratio $\|g^n\|_{L^2(Q_T)}/\|g^0\|_{L^2(Q_T)}$ with respect to the iterates and illustrates the remarkable robustness of the method.

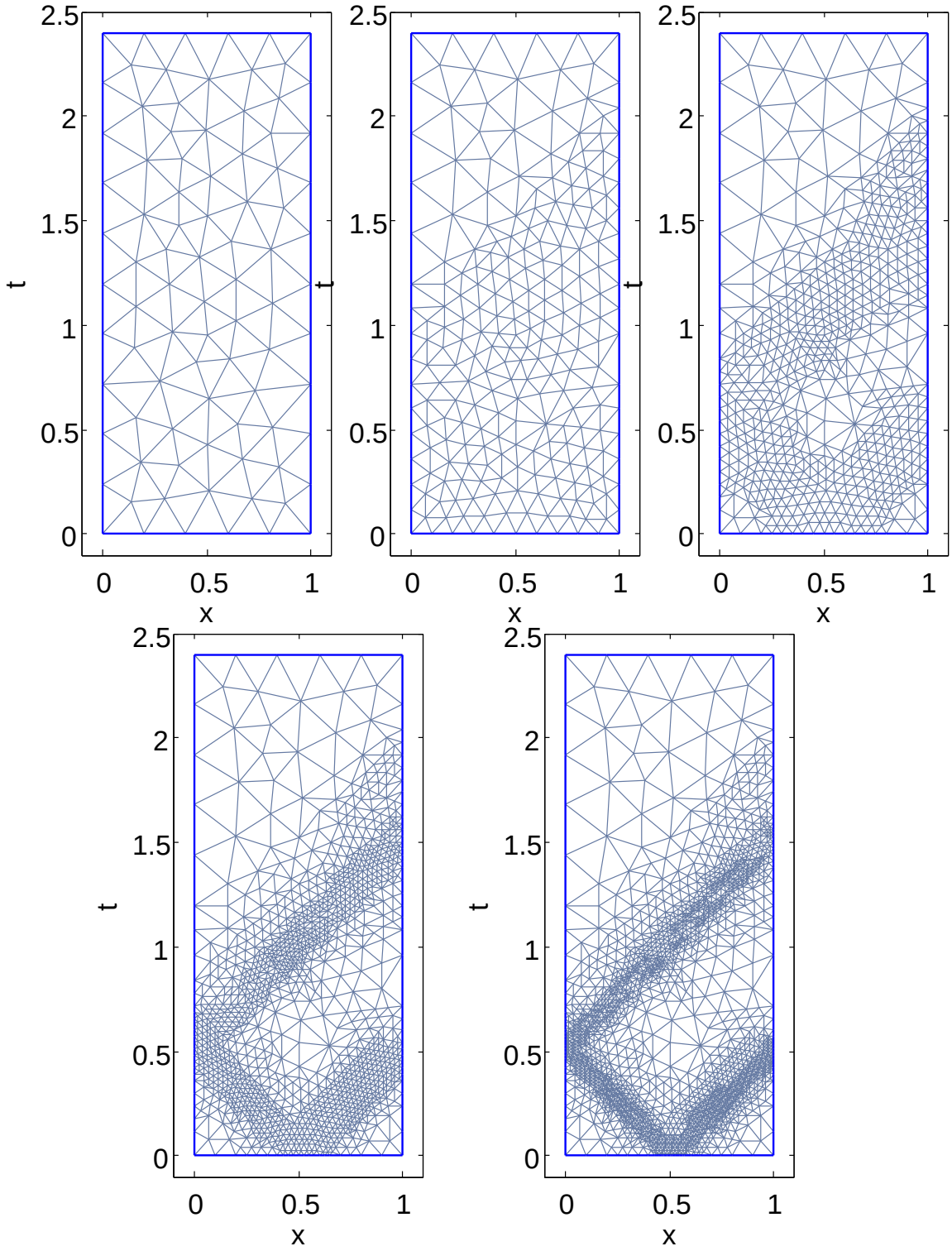

Figure 7: Example **EX3** - Iterative refinement of the triangular mesh over Q_T with respect to the variable λ_h: $142,412, 1\ 154, 2\ 556, 4\ 750$ triangles; $r = 2 \times 10^{-3}$.

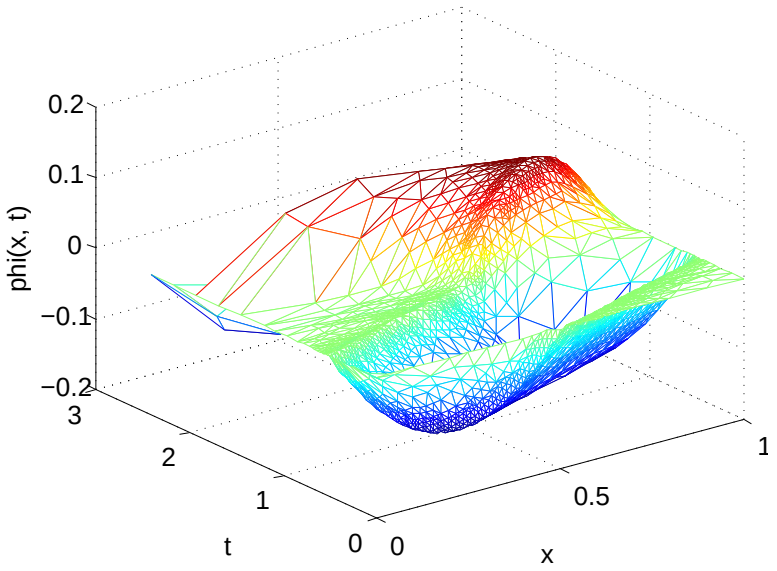

Figure 8: Example **EX3** : The dual variable φ_h in Q_T corresponding to the finer mesh of Figure 7; $r = 2 \times 10^{-3}$.

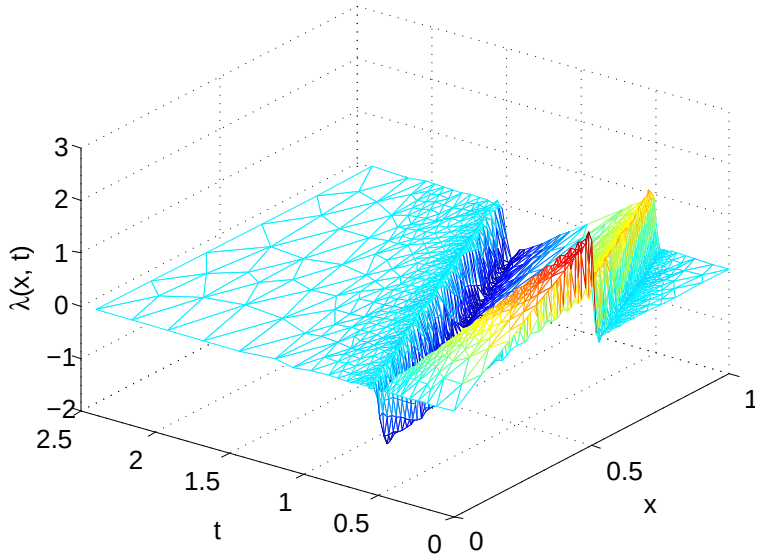

Figure 9: Example **EX3** : The primal variable λ_h in Q_T corresponding to the finer mesh of Figure 7.

h	1.56×10^{-1}	7.92×10^{-2}	3.99×10^{-2}	1.99×10^{-2}	9.99×10^{-3}
♯ iterates	37	62	83	101	105
$m_h = card(\{\lambda_h\})$	231	840	3 198	12 555	49 749
$\|\lambda_h(1,\cdot)\|_{L^2(0,T)}$	0.6452	0.6075	0.5902	0.5824	0.5790
$\|v - \lambda_h(1,\cdot)\|_{L^2(0,T)}$	2.87×10^{-1}	1.85×10^{-1}	1.25×10^{-1}	8.43×10^{-2}	6.02×10^{-2}
$\|\lambda_h\|_{L^2(Q_T)}$	0.6241	0.6001	0.5880	0.5822	0.5794

Table 17: Example **EX3** - BFS element - Conjugate gradient algorithm - $r = 10^{-2}$.

h	1.56×10^{-1}	7.92×10^{-2}	3.99×10^{-2}	1.99×10^{-2}	9.99×10^{-3}
♯ iterates	19	25	30	43	59
$\|\lambda_h(1,\cdot)\|_{L^2(0,T)}$	0.6089	0.5867	0.5857	0.5806	0.5784
$\|v - \lambda_h(1,\cdot)\|_{L^2(0,T)}$	2.41×10^{-1}	1.68×10^{-1}	1.28×10^{-1}	9.69×10^{-2}	7.62×10^{-2}
$\|\lambda_h\|_{L^2(Q_T)}$	0.6178	0.5963	0.5857	0.5806	0.5784

Table 18: Example **EX3** - BFS element - Conjugate gradient algorithm - $r = 1$.

h	1.56×10^{-1}	7.92×10^{-2}	3.99×10^{-2}	1.99×10^{-2}	9.99×10^{-3}
♯ iterates	15	20	23	32	44
$\|\lambda_h(1,\cdot)\|_{L^2(0,T)}$	0.4929	0.5365	0.5486	0.5577	0.5638
$\|v - \lambda_h(1,\cdot)\|_{L^2(0,T)}$	2.9×10^{-1}	2.18×10^{-1}	1.78×10^{-1}	1.43×10^{-1}	1.14×10^{-1}
$\|\lambda_h\|_{L^2(Q_T)}$	0.5957	0.5858	0.5797	0.5773	0.5763

Table 19: Example **EX3** - BFS element - Conjugate gradient algorithm - $r = 10^2$.

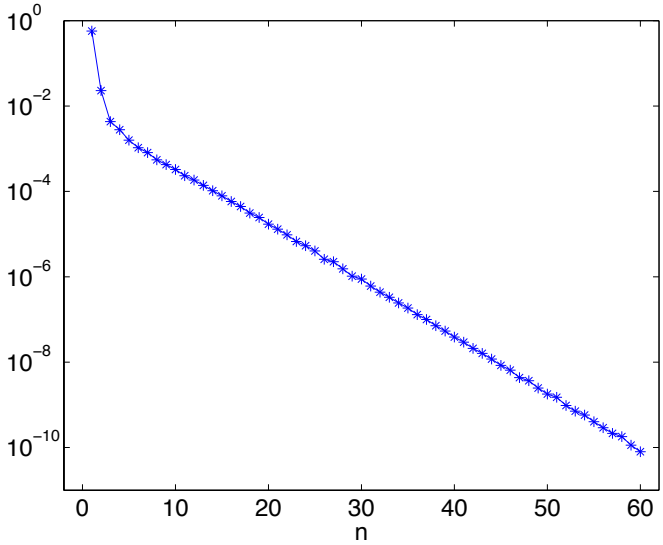

Figure 10: Example **EX3** : Evolution of $\|g^n\|_{L^2(Q_T)}/\|g^0\|_{L^2(Q_T)}$ w.r.t. the iterate n; $r = 1$; $h = 9.99 \times 10^{-3}$.

4.5 Numerical experiments: the inner case

We illustrate numerically the Section 3 which concerns the distributed controllability. Following Remark 2 and in order to avoid scalar product over H^{-1}, we solve the mixed formulation (35) and look for φ such that $L\varphi$ belongs to $L^2(Q_T)$. In this case, the numerical implementation of the distributed case is very similar to the boundary one : the term $\int_0^T c(1)\varphi_x(1,\cdot)\overline{\varphi}_x(1,\cdot)\,dt$ is simply replaced by the term $\iint_{q_T} \varphi\,\overline{\varphi}\,dx\,dt$. The other difference appears in the linear right hand side term of the mixed formulation due to the change of regularity of the initial data.

We consider the following data (see [11], Section 4.5):

$$\textbf{(EX4)} \qquad y_0(x) = e^{-500(x-0.2)^2}, \qquad y_1(x) = 0, \qquad T = 2.2, \qquad \omega = (0.2, 0.4)$$

and a non-constant function $c = c(x) \in C^1([0,1])$ with

$$c(x) = \begin{cases} 1. & x \in [0, 0.45] \\ \in [1., 5.] \quad (a'(x) > 0), & x \in (0.45, 0.55) \\ 5. & x \in [0.55, 1]. \end{cases} \tag{42}$$

We refine iteratively the mesh, using as before a criterion based on the gradient of λ_h. Figure 11 (left) depicts the mesh obtained after 3 iterations. Again, the characteristic lines, starting from $x = 0.2$ (where the initial position y_0 is mainly concentrated), may be observed on the figure. The corresponding approximation λ_h is represented on Figure 11 (right). For this simulation we have used $r = 2 \times 10^{-3}$. Table 20 gathers some informations on the successive meshes.

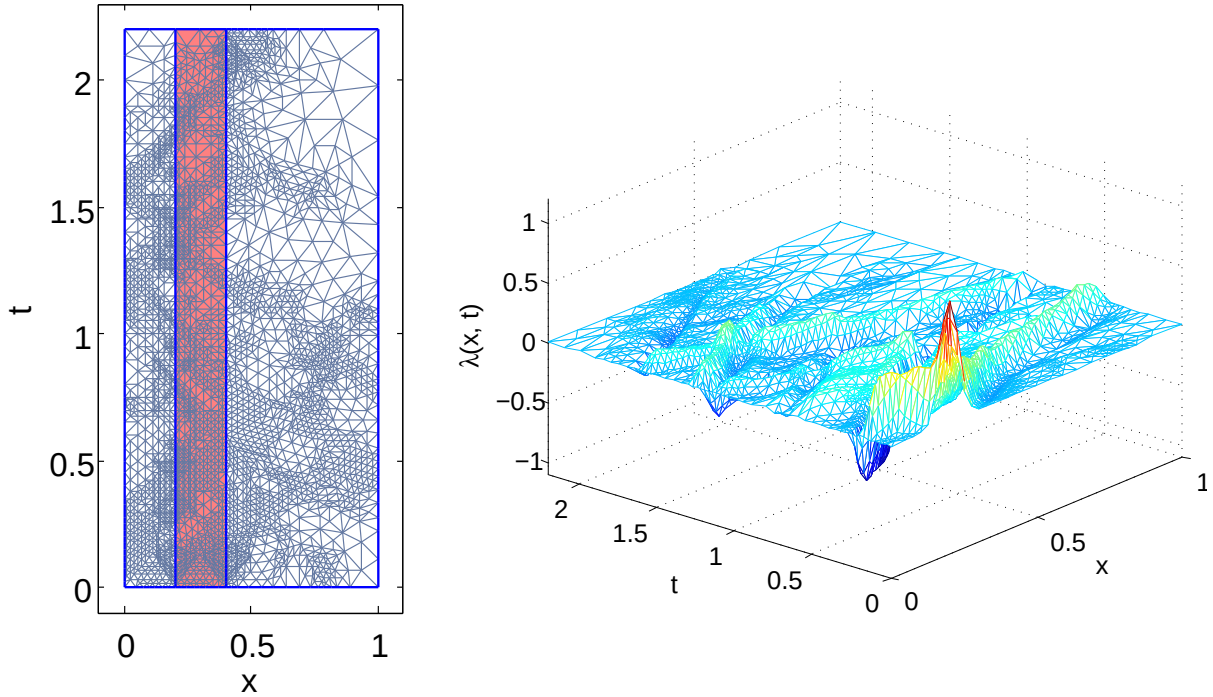

Figure 11: Example **EX4** : **Left :** Triangular mesh of q_T and of Q_T. **Right :** The primal variable λ_h in Q_T.

Iteration	0	1	2	3
♯ triangles	207	772	2 508	7 284
♯ points	120	415	1 300	3 710
$\|v_h\|_{L^2(q_T)}$	0.3703	0.3004	0.3573	0.4328

Table 20: Example **EX3** - Information on the successive meshes : the iterate 3 corresponds to the mesh of Figure 11.

5 Concluding remarks and perspectives

The mixed formulation we have introduced here in order to address the null controllability of the wave equation seems original. This formulation is nothing else than the Euler system associated to the conjugate functional and depends on both the dual adjoint variable and a Lagrange multiplier, which turns out to be the primal state of the wave equation to be controlled. The approach, recently used in a different way in [11], leads to a variational problem defined over time-space functional Hilbert spaces, without distinction between the time and the space variable. The main ingredients allowing to prove the well-posedness of the mixed formulation are an observability inequality, assuming here that T is large enough, and a direct inequality (also called the hidden regularity inequality). For these reasons, the mixed reformulation may also be employed to any other controllable systems for which such inequalities are available : we mention notably the parabolic case (in particular [16] where a variational approach is used for the heat equation), usually badly conditioned and for which direct robust methods are certainly very advantageous.

At the practical level, the discrete mixed time-space formulation is solved in a systematic way in the framework of the finite element theory: in contrast to the classical approach initially developed in [19], there is no need to take care of the time discretization nor of the stability of the resulting scheme, which is often a delicate issue. The resolution amounts to solve a sparse symmetric linear system : the corresponding matrix can be preconditioned if necessary, and may be computed once for all as it does not depend on the initial data to be controlled. Eventually, the space-time discretization of the domain allows an adaptation of the mesh so as to reduce the computational cost and capture the main features of the solutions.

For this reason, it is also worthwhile to remark that the variational approach developed here based on a space-time formulation allows to consider in a systematic way the case where the support of inner controls evolves in time. We refer to the work [6] where observability and controllability results are obtained for point-wise moving controls. Actually, using results from [6], we may extend the mixed formulation (35) and in particular prove, assuming T large enough, that the generalized observability inequality (36) also holds for control support of the form

$$q_T := \{(x,t) \in Q_T; \quad \gamma(t) - \gamma_1(t) < x < \gamma(t) + \gamma_2(t), \quad t \in (0,T)\}$$

where γ denotes any curve in the appropriate class defined in [6] and γ_1, γ_2 any functions in $C([0,T], \mathbb{R}_\star^+)$. This issue as well as the optimization of the domain q_T (leading to the control of minimal $L^2(q_T)$-norm, in the spirit of the work [32]) is fully discussed in [7].

Eventually, let us mention that upon classical conditions on the support of the control (distributed or located on a part of the boundary) and on the controllability time as discussed in [2, 27], the approach developed in this work remains valid in any dimension in space.

A Appendix: Numerical tables

h	1.41×10^{-1}	7.01×10^{-2}	3.53×10^{-2}	1.76×10^{-2}	8.83×10^{-3}
$\|\varphi - \varphi_h\|_{L^2(Q_T)}$	1.92×10^{-1}	1.71×10^{-2}	2.12×10^{-3}	2.8×10^{-4}	3.78×10^{-5}
$\|v - v_h\|_{L^2(0,T)}$	2.09×10^{-1}	7.19×10^{-2}	2.84×10^{-2}	1.05×10^{-2}	3.71×10^{-3}
$\|v_h\|_{L^2(0,T)}$	0.508	0.501	0.5	0.5	0.5
$\|L\varphi_h\|_{L^2(Q_T)}$	1.3×10^{2}	2.3×10^{1}	5.4×10^{0}	1.53×10^{0}	4.66×10^{-1}
$\|\lambda_h\|_{L^2(Q_T)}$	0.498	0.5	0.5	0.5	0.5
$\|\varphi_h\|_{\Phi}$	1.39	0.55	0.503	0.5	0.5
κ	4.28×10^{8}	2.64×10^{9}	2.5×10^{10}	3.7×10^{11}	6.91×10^{12}

Table 21: Example **EX1** - BFS element - $r = 10^{-4}$.

h	1.41×10^{-1}	7.01×10^{-2}	3.53×10^{-2}	1.76×10^{-2}	8.83×10^{-3}
$\|\varphi - \varphi_h\|_{L^2(Q_T)}$	2.6×10^{-3}	9.39×10^{-3}	4.08×10^{-4}	1.86×10^{-4}	8.86×10^{-5}
$\|v - v_h\|_{L^2(0,T)}$	5.32×10^{-2}	3.28×10^{-2}	1.88×10^{-2}	9.6×10^{-3}	4.48×10^{-3}
$\|v_h\|_{L^2(0,T)}$	0.4998	0.5	0.5	0.5	0.5
$\|L\varphi_h\|_{L^2(Q_T)}$	1.37	0.981	0.9042	0.9922	1.17
$\|\lambda_h\|_{L^2(Q_T)}$	0.4969	0.4997	0.4999	0.4999	0.5
$\|\varphi_h\|_{\Phi}$	0.5182	0.5026	0.5	0.5	0.5
κ	5.47×10^{7}	9.64×10^{8}	1.81×10^{10}	3.56×10^{11}	7.19×10^{12}

Table 22: Example **EX1** - BFS element - $r = h^2$.

h	1.41×10^{-1}	7.01×10^{-2}	3.53×10^{-2}	1.76×10^{-2}	8.83×10^{-3}
$\|\varphi - \varphi_h\|_{L^2(Q_T)}$	2.11×10^{-2}	1.35×10^{-2}	1.35×10^{-3}	8.86×10^{-5}	5.60×10^{-6}
$\|v - v_h\|_{L^2(Q_T)}$	4.18×10^{-1}	1.83×10^{-1}	1.81×10^{-2}	1.18×10^{-3}	7.47×10^{-5}
$\|v_h\|_{L^2(Q_T)}$	0.049	0.312	0.481	0.498	0.5
$\|L\varphi_h\|_{L^2(Q_T)}$	1.49×10^{-2}	2.4×10^{-2}	9.3×10^{-3}	2.4×10^{-3}	6.1×10^{-4}
$\|\lambda_h\|_{L^2(Q_T)}$	0.408	0.446	0.493	0.499	0.5
$\|\varphi_h\|_{\Phi}$	0.157	0.395	0.493	0.499	0.5
κ	2.92×10^{11}	1.57×10^{13}	1.06×10^{15}	6.92×10^{16}	4.44×10^{18}

Table 23: Example **EX1** - BFS element - $r = 10^2$.

h	1.41×10^{-1}	7.01×10^{-2}	3.53×10^{-2}	1.76×10^{-2}	8.83×10^{-3}
$\|\varphi - \varphi_h\|_{L^2(Q_T)}$	3.2×10^{-2}	3.34×10^{-2}	2.8×10^{-2}	1.62×10^{-2}	6.06×10^{-3}
$\|v - v_h\|_{L^2(0,T)}$	4.5×10^{-1}	4.53×10^{-1}	3.75×10^{-1}	2.8×10^{-1}	8.06×10^{-2}
$\|v_h\|_{L^2(0,T)}$	0.01	0.03	0.12	0.2824	0.4192
$\|L\varphi_h\|_{L^2(Q_T)}$	2.21×10^{-2}	4.16×10^{-2}	6.8×10^{-2}	7.8×10^{-2}	5.81×10^{-2}
$\|\lambda_h\|_{L^2(Q_T)}$	0.443	0.44	0.435	0.4459	0.4753
κ	2.17×10^{10}	4.92×10^{11}	1.38×10^{13}	4.06×10^{14}	1.46×10^{19}

Table 24: Example **EX1** - HCT element - Uniform mesh - $r = 10$.

h	1.41×10^{-1}	7.01×10^{-2}	3.53×10^{-2}	1.76×10^{-2}	8.83×10^{-3}
$\|\varphi - \varphi_h\|_{L^2(Q_T)}$	3.69×10^{-3}	1.07×10^{-3}	4.33×10^{-4}	1.91×10^{-4}	3.79×10^{-4}
$\|v - v_h\|_{L^2(0,T)}$	5.26×10^{-2}	2.24×10^{-2}	9.23×10^{-3}	3.76×10^{-3}	1.56×10^{-3}
$\|v_h\|_{L^2(0,T)}$	0.4773	0.4988	0.4999	0.5	0.5
$\|L\varphi_h\|_{L^2(Q_T)}$	1.78	0.1424	0.9347	0.9784	4.9939
$\|\lambda_h\|_{L^2(Q_T)}$	0.4938	0.5003	0.5002	0.5	0.5
κ	2.85×10^{5}	1.83×10^{6}	1.57×10^{7}	1.08×10^{8}	9.43×10^{8}

Table 25: Example **EX1** - HCT element - Uniform mesh - $r = h^2$.

h	1.41×10^{-1}	7.01×10^{-2}	3.53×10^{-2}	1.76×10^{-2}	8.83×10^{-3}
$\|\varphi - \varphi_h\|_{L^2(Q_T)}$	2.18×10^{-1}	2.13×10^{-2}	2.43×10^{-3}	2.94×10^{-4}	3.56×10^{-5}
$\|v - v_h\|_{L^2(0,T)}$	1.77×10^{-1}	3.08×10^{-2}	1.05×10^{-2}	3.87×10^{-3}	1.42×10^{-3}
$\|v_h\|_{L^2(0,T)}$	0.5273	0.5007	0.5001	0.5	0.5
$\|L\varphi_h\|_{L^2(Q_T)}$	131.39	24.11	5.51	1.52	4.49×10^{-1}
$\|\lambda_h\|_{L^2(Q_T)}$	0.5046	0.5005	0.5002	0.5001	0.5
κ	7.22×10^{5}	2.76×10^{6}	1.53×10^{7}	1.12×10^{8}	8.87×10^{8}

Table 26: Example **EX1** - HCT element - Uniform mesh - $r = 10^{-4}$.

h	9.02×10^{-2}	4.51×10^{-2}	2.55×10^{-2}	1.13×10^{-2}	5.6×10^{-3}
$\|\varphi - \varphi_h\|_{L^2(Q_T)}$	2.15×10^{-2}	9.8×10^{-3}	2.93×10^{-3}	7.64×10^{-4}	1.93×10^{-4}
$\|v - v_h\|_{L^2(0,T)}$	2.75×10^{-1}	1.24×10^{-1}	3.74×10^{-2}	1.006×10^{-2}	2.71×10^{-3}
$\|v_h\|_{L^2(0,T)}$	0.1898	0.3674	0.461	0.4899	0.4974
$\|L\varphi_h\|_{L^2(Q_T)}$	0.2421	0.2204	0.1339	0.0701	0.0353
$\|\lambda_h\|_{L^2(Q_T)}$	0.4317	0.4687	0.4894	0.4971	0.4992
κ	1.45×10^{9}	4.15×10^{10}	1.25×10^{12}	5×10^{13}	1.28×10^{15}

Table 27: Example **EX1** - HCT element - Non uniform mesh - $r = 1$.

h	9.02×10^{-2}	4.51×10^{-2}	2.55×10^{-2}	1.13×10^{-2}	5.6×10^{-3}
$\|\varphi - \varphi_h\|_{L^2(Q_T)}$	1.24×10^{-3}	1.69×10^{-4}	3.47×10^{-5}	8.07×10^{-6}	1.98×10^{-6}
$\|v - v_h\|_{L^2(0,T)}$	3.79×10^{-2}	1.02×10^{-2}	2.59×10^{-3}	6.47×10^{-4}	1.53×10^{-4}
$\|v_h\|_{L^2(0,T)}$	0.4915	0.4981	0.4996	0.4999	0.5
$\|L\varphi_h\|_{L^2(Q_T)}$	1.2064	0.3612	0.1536	0.0729	0.0357
$\|\lambda_h\|_{L^2(Q_T)}$	0.4981	0.4996	0.4999	0.5	0.5
κ	2.76×10^{6}	3.28×10^{7}	4.12×10^{8}	8.78×10^{9}	1.77×10^{11}

Table 28: Example **EX1** - HCT element - Non uniform mesh - $r = 10^{-2}$.

h	1.41×10^{-1}	7.01×10^{-2}	3.53×10^{-2}	1.76×10^{-2}	8.83×10^{-3}
$\|v_h\|_{L^2(0,T)}$	0.4551	0.4723	0.4982	0.5177	0.5274
$\|v - v_h\|_{L^2(0,T)}$	2.31×10^{-1}	1.71×10^{-1}	1.06×10^{-1}	6.48×10^{-2}	3.91×10^{-2}
$\|\lambda_h\|_{L^2(Q_T)}$	0.5331	0.5232	0.5254	0.5299	0.5325
$\|L\varphi_h\|_{L^2(Q_T)}$	1.52×10^{-1}	1.4×10^{-1}	1.18×10^{-1}	8.34×10^{-2}	5.51×10^{-2}

Table 29: Example **EX2** - HCT element - Uniform mesh - $r = 1$.

h	1.41×10^{-1}	7.01×10^{-2}	3.53×10^{-2}	1.76×10^{-2}	8.83×10^{-3}
$\|v_h\|_{L^2(0,T)}$	0.5496	0.537	0.5345	0.5342	0.5344
$\|v - v_h\|_{L^2(0,T)}$	5.05×10^{-2}	2.73×10^{-2}	1.69×10^{-2}	1.09×10^{-2}	6.8×10^{-3}
$\|\lambda_h\|_{L^2(Q_T)}$	0.5557	0.5407	0.5361	0.5349	0.5346
$\|L\varphi_h\|_{L^2(Q_T)}$	2.0168	7.53×10^{-1}	3.53×10^{-1}	1.97×10^{-1}	1.16×10^{-1}

Table 30: Example **EX2** - HCT element - Uniform mesh - $r = 10^{-2}$.

h	1.41×10^{-1}	7.01×10^{-2}	3.53×10^{-2}	1.76×10^{-2}	8.83×10^{-3}
$\|v_h\|_{L^2(0,T)}$	0.626	0.600	0.587	0.581	0.578
$\|v - v_h\|_{L^2(0,T)}$	3.2×10^{-1}	2.26×10^{-1}	1.56×10^{-1}	1.07×10^{-1}	7.49×10^{-2}
$\|\lambda_h\|_{L^2(Q_T)}$	0.626	0.601	0.588	0.582	0.579
$\|L\varphi_h\|_{L^2(Q_T)}$	2.83×10^{0}	1.71×10^{0}	1.02×10^{0}	6.13×10^{-1}	3.82×10^{-1}

Table 31: Example **EX3** - BFS element - $r = 10^{-2}$.

h	1.56×10^{-1}	7.81×10^{-2}	3.90×10^{-2}	1.95×10^{-2}	9.76×10^{-3}
$\|v_h\|_{L^2(0,T)}$	0.6044	0.5864	0.576	0.5595	0.5716
$\|v - v_h\|_{L^2(Q_T)}$	2.55×10^{-1}	1.3×10^{-1}	8.7×10^{-2}	7.81×10^{-2}	7.27×10^{-2}
$\|\lambda_h\|_{L^2(Q_T)}$	0.619	0.5955	0.5806	0.5722	0.5774
$\|L\varphi_h\|_{L^2(Q_T)}$	2.7028	1.6157	1.0384	7.3×10^{-1}	5.77×10^{-1}

Table 32: Example **EX3** - HCT element - Uniform mesh - $r = 10^{-2}$.

h	9.87×10^{-2}	4.93×10^{-2}	2.46×10^{-2}	1.23×10^{-2}	6.17×10^{-3}
$\|v_h\|_{L^2(0,T)}$	0.612	0.584	0.5746	0.5715	0.5713
$\|v - v_h\|_{L^2(0,T)}$	2.45×10^{-1}	1.57×10^{-1}	1.15×10^{-1}	1.08×10^{-1}	8.84×10^{-2}
$\|\lambda_h\|_{L^2(Q_T)}$	0.6203	0.5976	0.5857	0.5802	0.5779
$\|L\varphi_h\|_{L^2(Q_T)}$	2.8835	1.6143	9.71×10^{-1}	6.43×10^{-1}	4.68×10^{-1}

Table 33: Example **EX3** - HCT element - Non uniform mesh - $r = 10^{-2}$.

References

[1] M. Asch and G. Lebeau, *Geometrical aspects of exact boundary controllability for the wave equation—a numerical study*, ESAIM Control Optim. Calc. Var., 3 (1998), pp. 163–212 (electronic).

[2] C. Bardos, G. Lebeau, and J. Rauch, *Sharp sufficient conditions for the observation, control, and stabilization of waves from the boundary*, SIAM J. Control Optim., 30 (1992), pp. 1024–1065.

[3] M. Bernadou and K. Hassan, *Basis functions for general Hsieh-Clough-Tocher triangles, complete or reduced*, Internat. J. Numer. Methods Engrg., 17 (1981), pp. 784–789.

[4] F. Bourquin, *Approximation theory for the problem of exact controllability of the wave equation with boundary control*, in Second International Conference on Mathematical and Numerical Aspects of Wave Propagation (Newark, DE, 1993), SIAM, Philadelphia, PA, 1993, pp. 103–112.

[5] F. Brezzi and M. Fortin, *Mixed and hybrid finite element methods*, vol. 15 of Springer Series in Computational Mathematics, Springer-Verlag, New York, 1991.

[6] C. Castro, *Exact controllability of the 1-D wave equation from a moving interior point*, ESAIM Control Optim. Calc. Var., 19 (2013), pp. 301–316.

[7] C. Castro, N. Cîndea, and A. Münch, *Controllability of the linear wave equation with moving inner actions.*, (in prep.).

[8] C. Castro, S. Micu, and A. Münch, *Numerical approximation of the boundary control for the wave equation with mixed finite elements in a square*, IMA J. Numer. Anal., 28 (2008), pp. 186–214.

[9] D. Chapelle and K.-J. Bathe, *The inf-sup test*, Comput. & Structures, 47 (1993), pp. 537–545.

[10] P. G. Ciarlet, *The finite element method for elliptic problems*, vol. 40 of Classics in Applied Mathematics, Society for Industrial and Applied Mathematics (SIAM), Philadelphia, PA, 2002. Reprint of the 1978 original [North-Holland, Amsterdam; MR0520174 (58 #25001)].

[11] N. Cîndea, E. Fernández-Cara, and A. Münch, *Numerical controllability of the wave equation through primal methods and Carleman estimates*, ESAIM COCV, 19 (2013).

[12] N. Cîndea, S. Micu, and M. Tucsnak, *An approximation method for exact controls of vibrating systems*, SIAM J. Control Optim., 49 (2011), pp. 1283–1305.

[13] J. W. Daniel, *The approximate minimization of functionals*, Prentice-Hall Inc., Englewood Cliffs, N.J., 1971.

[14] D. A. Dunavant, *High degree efficient symmetrical Gaussian quadrature rules for the triangle*, Internat. J. Numer. Methods Engrg., 21 (1985), pp. 1129–1148.

[15] S. Ervedoza and E. Zuazua, *On the numerical approximation of exact controls for waves*, vol. XVII of Springer Briefs in Mathematics, 2013.

[16] E. Fernández-Cara and A. Münch, *Strong convergence approximations of null controls for the 1D heat equation*, SēMA J., 61 (2013), pp. 49–78.

[17] M. Fortin and R. Glowinski, *Augmented Lagrangian methods*, vol. 15 of Studies in Mathematics and its Applications, North-Holland Publishing Co., Amsterdam, 1983. Applications to the numerical solution of boundary value problems, Translated from the French by B. Hunt and D. C. Spicer.

[18] R. Glowinski, *Handbook of numerical analysis. Vol. IX*, Handbook of Numerical Analysis, IX, North-Holland, Amsterdam, 2003. Numerical methods for fluids. Part 3.

[19] R. Glowinski and J.-L. Lions, *Exact and approximate controllability for distributed parameter systems*, in Acta numerica, 1995, Acta Numer., Cambridge Univ. Press, Cambridge, 1995, pp. 159–333.

[20] R. Glowinski, J.-L. Lions, and J. He, *Exact and approximate controllability for distributed parameter systems*, vol. 117 of Encyclopedia of Mathematics and its Applications, Cambridge University Press, Cambridge, 2008. A numerical approach.

[21] M. Gunzburger, L. S. Hou, and L. Ju, *A numerical method for exact boundary controllability problems for the wave equation*, Comput. Math. Appl., 51 (2006), pp. 721–750.

[22] L. Ju, M. D. Gunzburger, and L. S. Hou, *Approximation of exact boundary controllability problems for the 1-D wave equation by optimization-based methods*, in Recent advances in scientific computing and partial differential equations (Hong Kong, 2002), vol. 330 of Contemp. Math., Amer. Math. Soc., Providence, RI, 2003, pp. 133–153.

[23] V. Komornik, *Exact controllability and stabilization*, RAM: Research in Applied Mathematics, Masson, Paris, 1994. The multiplier method.

[24] V. Komornik and P. Loreti, *Observability of discretized wave equations*, Bol. Soc. Parana. Mat. (3), 25 (2007), pp. 67–76.

[25] I. Lasiecka, R. Triggiani, and P. F. Yao, *Exact controllability for second-order hyperbolic equations with variable coefficient-principal part and first-order terms*, in Proceedings of the Second World Congress of Nonlinear Analysts, Part 1 (Athens, 1996), vol. 30, 1997, pp. 111–122.

[26] G. Lebeau and M. Nodet, *Experimental study of the HUM control operator for linear waves*, Experiment. Math., 19 (2010), pp. 93–120.

[27] J.-L. Lions, *Contrôlabilité exacte, perturbations et stabilisation de systèmes distribués. Tome 1*, vol. 8 of Recherches en Mathématiques Appliquées [Research in Applied Mathematics], Masson, Paris, 1988. Contrôlabilité exacte. [Exact controllability], With appendices by E. Zuazua, C. Bardos, G. Lebeau and J. Rauch.

[28] P. Loreti and M. Mehrenberger, *An Ingham type proof for a two-grid observability theorem*, ESAIM Control Optim. Calc. Var., 14 (2008), pp. 604–631.

[29] A. Meyer, *A simplified calculation of reduced hct-basis functions in a finite element context*, Comput. Methods Appl. Math., 12 (2012), pp. 486–499.

[30] A. Münch, *A uniformly controllable and implicit scheme for the 1-D wave equation*, M2AN Math. Model. Numer. Anal., 39 (2005), pp. 377–418.

[31] P. Pedregal, F. Periago, and J. Villena, *A numerical method of local energy decay for the boundary controllability of time-reversible distributed parameter systems*, Stud. Appl. Math., 121 (2008), pp. 27–47.

[32] F. Periago, *Optimal shape and position of the support for the internal exact control of a string*, Systems Control Lett., 58 (2009), pp. 136–140.

[33] P.-F. Yao, *On the observability inequalities for exact controllability of wave equations with variable coefficients*, SIAM J. Control Optim., 37 (1999), pp. 1568–1599.

[34] X. Zhang, *Explicit observability estimate for the wave equation with potential and its application*, R. Soc. Lond. Proc. Ser. A Math. Phys. Eng. Sci., 456 (2000), pp. 1101–1115.